Journal of Visualized Experiments

Protocol for in vivo calcium imaging of lateral-line hair cells in larval zebrafish.
--Manuscript Draft--

Article Type:	Invited Methods Article - JoVE Produced Video
Manuscript Number:	JoVE58794R1
Full Title:	Protocol for in vivo calcium imaging of lateral-line hair cells in larval zebrafish.
Keywords:	zebrafish; hair cells; GCaMP; calcium imaging; in vivo; mechanosensation; synapse
Corresponding Author:	Katie Kindt National Institutes of Health Bethesda, UNITED STATES
Corresponding Author's Institution:	National Institutes of Health
Corresponding Author E-Mail:	katie.kindt@nih.gov
Order of Authors:	Katie Kindt
	Daria Lukasz
Additional Information:	
Question	**Response**
Please indicate whether this article will be Standard Access or Open Access.	Open Access (US$4,200)
Please indicate the **city, state/province, and country** where this article will be **filmed**. Please do not use abbreviations.	Bethesda, MD, USA

Katie Kindt
National Institute on Deafness
and Other Communication Disorders

Bethesda, Maryland 20814
Building: 35A
Room: 1D-933
(v) (301) 443-2626
(email) katie.kindt@nidcd.nih.gov

August 23th, 2018

Dear Dr. Myers,

Please find enclosed our revised manuscript entitled **"Protocol for *in vivo* calcium imaging of lateral-line hair cells in larval zebrafish."** This manuscript presents a cutting edge *in vivo* method that we have used successfully to study the function of hair cells, the sensory cells required for hearing and balance.

In our revised manuscript, we have incorporated the excellent advice of both reviewers and the reviewing editor.

In its current form, we feel our revised work is now suitable for publication in JoVE.

Please see the attached document where we have addressed the concerns of each reviewer, in a point-by-point manner.

Thank you for re-considering our manuscript,

Sincerely,

Katie Kindt

1   **TITLE:**
2   *In Vivo* Calcium Imaging of Lateral-line Hair Cells in Larval Zebrafish
3
4   **AUTHORS AND AFFILIATIONS:**
5   Daria Lukasz[1,2], Katie S. Kindt[1]
6
7   [1]Section on Sensory Cell Development and Function, NIDCD/National Institutes of Health,
8   Bethesda, MD, USA
9   [2]National Institutes of Health–Johns Hopkins University Graduate Partnerships Program,
10   Baltimore, MD, USA
11
12   **Corresponding Author:**
13   Katie S. Kindt   (Katie.kindt@nih.gov)
14
15   **Email Address of Co-author:**
16   Daria Lukasz   (Daria.lukasz@nih.gov)
17

18   **KEYWORDS:**
19   Zebrafish, calcium imaging, confocal imaging, *in vivo* imaging, hair cells, sensory neuroscience,
20   lateral line, genetically encoded indicators, GCaMP
21

22   **SUMMARY:**
23   The zebrafish is a model system that has many valuable features including optical clarity, rapid
24   external development, and, of particular importance to the field of hearing and balance,
25   externally located sensory hair cells. This article outlines how transgenic zebrafish can be used to
26   assay both hair-cell mechanosensation and presynaptic function *in toto*.
27

28   **ABSTRACT:**
29   Sensory hair cells are mechanoreceptors found in the inner ear that are required for hearing and
30   balance. Hair cells are activated in response to sensory stimuli that mechanically deflect apical
31   protrusions called hair bundles. Deflection opens mechanotransduction (MET) channels in hair
32   bundles, leading to an influx of cations, including calcium. This cation influx depolarizes the cell
33   and opens voltage-gated calcium channels located basally at the hair-cell presynapse. In
34   mammals, hair cells are encased in bone, and it is challenging to functionally assess these
35   activities *in vivo*. In contrast, larval zebrafish are transparent and possess an externally located
36   lateral-line organ that contains hair cells. These hair cells are functionally and structurally similar
37   to mammalian hair cells and can be functionally assessed *in vivo*. This article outlines a technique
38   that utilizes a genetically encoded calcium indicator (GECI), GCaMP6s, to measure stimulus-
39   evoked calcium signals in zebrafish lateral-line hair cells. GCaMP6s can be used, along with
40   confocal imaging, to measure *in vivo* calcium signals at the apex and base of lateral-line hair cells.
41   These signals provide a real-time, quantifiable readout of both mechanosensation- and
42   presynapse-dependent calcium activities within these hair cells. These calcium signals also
43   provide important functional information regarding how hair cells detect and transmit sensory
44   stimuli. Overall, this technique generates useful data about relative changes in calcium activity *in*

45 *vivo*. It is less well-suited for quantification of the absolute magnitude of calcium changes. This *in*
46 *vivo* technique is sensitive to motion artifacts. A reasonable amount of practice and skill are
47 required for proper positioning, immobilization, and stimulation of larvae. Ultimately, when
48 properly executed, the protocol outlined in this article provides a powerful way to collect
49 valuable information about the activity of hair-cells in their natural, fully integrated states within
50 a live animal.
51
52 **INTRODUCTION:**
53 Functional calcium imaging is a powerful tool that can be used to monitor the activity of many
54 cells simultaneously[1]. In particular, calcium imaging using genetically encoded calcium indicators
55 (GECIs) has been shown to be advantageous because GECIs can be expressed in specific cell types
56 and localized subcellularly[2]. In neuroscience research, these features have made calcium imaging
57 using GECIs a powerful method to both define activity patterns within neuronal networks and
58 measure calcium influx at individual synapses[3,4]. Taking advantage of these features, a recent
59 study used confocal microscopy and GECIs to monitor subcellular activity within collections of
60 sensory hair cells[5].
61
62 Hair cells are the mechanoreceptors that detect sound and vestibular stimuli in the inner ear and
63 local water movement in the lateral-line system in aquatic vetebrates[6,7]. Hair cells are often the
64 target of damage or genetic mutations that result in the most common form of hearing loss in
65 humans known as sensorineural hearing loss[8,9]. Therefore, it is critical to understand how these
66 cells function in order to understand how to treat and prevent hearing loss. To properly function,
67 hair cells utilize two specialized structures called mechanosensory-hair bundles and synaptic
68 ribbons to detect and transmit stimuli, respectively. Hair bundles are located at the apex of hair
69 cells and are made up primarily of fine, hair-like protrusions known as stereocilia (**Figure 1A**). In
70 vestibular and lateral-line hair cells, each hair bundle also has a single long kinocilium (the cell's
71 only true cilium), which can extend far above the stereocilia (**Figure 1A**). Mechanosensory stimuli
72 deflect hair bundles, and deflection puts tension on linkages called "tip-links" that interconnect
73 stereocilia[10]. This tension opens mechanotransduction (MET) channels located in the stereocilia,
74 resulting in an apical influx of cations, including calcium[11,12]. This apical activity ultimately
75 depolarizes the hair cell and opens voltage-gated calcium channels ($Ca_v1.3$) at the base of the
76 cell. $Ca_v1.3$ channels are found adjacent to synaptic ribbons, a presynaptic structure that tethers
77 vesicles at active zones. Basal calcium influx through $Ca_v1.3$ channels is required for vesicle fusion,
78 neurotransmission, and activation of afferent neurons[13,14].
79
80 For many years, electrophysiological techniques such as whole-cell patch clamping have been
81 used to probe the functional properties of hair cells in many species, including zebrafish[15-20].
82 These electrophysiological recordings have been particularly valuable in the hearing and balance
83 fields because they can be used to obtain extremely sensitive measurements from individual
84 sensory cells, whose purpose is to encode extremely fast stimuli over a wide range of frequencies
85 and intensities[21,22]. Unfortunately, whole-cell recordings cannot measure the activity of
86 populations of hair cells. To study the activity of populations of cells in the zebrafish lateral-line,
87 microphonic potentials and afferent action potentials have been used to measure the summed
88 mechanosensitive and postsynaptic response properties of individual neuromasts[23,24].

89   Unfortunately, neither whole-cell recordings nor local field potential measurements have the
90   spatial resolution to pinpoint where activity is occurring within individual cells or measure the
91   activity of each cell within a population. More recently, calcium dyes and GECIs have been
92   employed to bypass these challenges[25,26].
93
94   In zebrafish, GECIs have proven to be a powerful approach to examining hair-cell function due to
95   the relative ease of creating transgenic zebrafish and the optical clarity of larvae[27]. In zebrafish
96   larvae, hair cells are present in the inner ear as well as the lateral-line system. The lateral line is
97   made up of rosette-like clusters of hair cells called neuromasts that are used to detect local
98   changes in water movement (**Figure 1**). The lateral line is particularly useful because it is located
99   externally along the surface of the fish. This access has made it possible to stimulate hair cells
100 and measure calcium signals optically in intact larvae. Overall, the ease of transgenesis,
101 transparency of the larvae, and the unparalleled access of lateral-line hair cells have made
102 zebrafish an invaluable model to study the activity of hair cells *in vivo*. This is a significant
103 advantage compared to mammalian systems in which hair cells are surrounded by bony
104 structures of the inner ear. This lack of access has made it very difficult to acquire functional *in*
105 *vivo* measurements of mammalian hair cells.
106
107 The protocol outlined here describes how to monitor MET channel- and presynapse-dependent
108 changes in calcium within individual hair cells and among cells within neuromasts in larval
109 zebrafish. This protocol utilizes an established transgenic zebrafish line that expresses a
110 membrane-localized GCaMP6s under the control of the hair-cell specific *myosin6b* promoter[28].
111 This membrane localization positions GCaMP6s to detect calcium influx through ion channels
112 located in the plasma membrane that are critical for hair-cell function. For example, membrane-
113 localized GCaMP6s can detect calcium influx through MET channels in apical hair bundles and
114 through $Ca_V1.3$ channels near synaptic ribbons at the base of the cell. This contrasts with using
115 GECIs localized in the cytosol, as cytosolic GECIs detect calcium signals that are a combination of
116 MET and $Ca_V1.3$ channel activity as well as calcium contributions from other sources (*e.g.,* store
117 release). This protocol outlines how to immobilize and paralyze GCaMP6s transgenic larvae prior
118 to imaging. It then describes how to prepare and use a fluid-jet to deflect the hair bundles to
119 stimulate lateral-line hair cells in a controlled and reproducible manner. Representative data that
120 can be achieved using this protocol are presented. Examples of data that represent movement
121 artifacts are also presented. Control experiments that are used to verify results and exclude
122 artifacts are described. Lastly, a method to visualize spatial calcium signals in the Fiji software is
123 described. This Fiji analysis is adapted from previously established visualization methods
124 developed using MATLAB[5]. Overall, this protocol outlines a powerful preparation technique that
125 uses GECIs in larval zebrafish to measure and visualize hair-cell calcium dynamics *in vivo*.
126
127 **PROTOCOL:**
128 All animal work was approved by the Animal Use Committee at the National Institutes of Health
129 under animal study protocol #1362-13.
130
131 Note: This protocol takes approximately 0.5-1 h to complete with no interruptions if the solutions
132 and equipment are prepared and set up in advance. This protocol is optimized for

133 Tg(myo6b:GCaMP6s-caax)[5,29] zebrafish larvae at 3-7 days post-fertilization (dpf). This transgenic
134 line expresses a membrane-localized GCaMP6s (zebrafish codon-optimized) specifically in all
135 zebrafish hair cells. Prior to imaging, larvae are raised in the embryo buffer (E3) under standard
136 conditions. Refer to the **Table of Materials** for catalog numbers of all equipment and drugs
137 required to execute this protocol.
138
139 **1.   Preparation of Solutions**
140
141 1.1.   Prepare 1 mL of α-bungarotoxin (125 µM), which is used to paralyze zebrafish larvae
142 during functional imaging.
143
144 1.1.1.   Add 968.6 µL of ultrapure sterile water and 33.4 µL of phenol red to 1 mg of α-
145 bungarotoxin (entire bottle). Make 100 µL aliquots and store them at -20 °C.
146
147 CAUTION: Wear gloves and make preparations in the hood when handling α-bungarotoxin
148 powder. Gloves are also recommended when handling the α-bungarotoxin solution.
149
150 1.2.   Prepare 1 L of 60x embryo buffer (E3).
151
152 1.2.1.   Add 17.2 g of NaCl and 0.76 g of KCl powder to 954.4 mL of ultrapure water.
153
154 1.2.2.   Add 19.8 mL of 1 M $CaCl_2$, 19.8 mL of 1 M $MgSO_4$, and 6 mL of 1 M HEPES buffer to the
155 solution. Store the 60x E3 stock solution at 4 °C for up to 6 months.
156
157 1.3.   Prepare 10 L of 1x E3 (5 mM NaCl; 0.17 mM KCl; 0.33 mM $CaCl_2$; 0.33 mM $MgSO_4$, pH 7.2),
158 which is a solution that larvae are propagated in prior to functional imaging.
159
160 1.3.1.   Add 167 mL of 60x E3 stock solution to 10 L of ultrapure water to make a 1x E3 solution.
161 Store the 1x E3 solution at room temperature (RT) for up to 6 months.
162
163 1.4.   Prepare neuronal buffer (NB) (140 mM NaCl; 2 mM KCl; 2 mM $CaCl_2$; 1 mM $MgCl_2$; 10 mM
164 HEPES buffer, pH 7.3), which is used to immerse larvae during functional imaging.
165
166 Note: 1x E3 can also be used for functional imaging, but responses are more robust and reliable
167 in NB.
168
169 1.4.1.   Combine 28 mL of 5 M NaCl, 2 mL of 1 M KCl, 2 mL of 1 M $CaCl_2$, 1 mL of 1 M $MgCl_2$, and
170 10 mL of 1 M HEPES buffer with 957 mL of ultrapure water. Bring the pH to 7.3 with 1 M NaOH.
171
172 1.4.2.   Filter sterilize. Store at 4 °C for up to 1 month.
173
174 Note: Bring to RT before using solution.
175
176 1.5.   Prepare MS-222 stock (tricaine, 0.4%), which is used to anesthetize larvae.

177

1.5.1. Dissolve 400 mg of ethyl 3-aminobenzoate methanesulfonate salt and 800 mg of Na_2HPO_4 in 100 mL of distilled water. Adjust the pH to 7. Store at 4 °C.

1.5.2. Use 0.04% MS-222 to anesthetize larvae during immobilization and α-bungarotoxin injection.

2. Preparation of Imaging Chamber and Pins

2.1.   Prepare the imaging chamber (**Figure 2A**). Apply a thin layer of high vacuum silicone grease to the bottom of the perfusion chamber along the edges of the square to which the coverslip will adhere. Do not leave gaps in the grease. Firmly press down around the edges of the coverslip to seal it to the imaging chamber. Wipe away excess grease.

Note: A 5 mL syringe with a 200 µL micropipette tip is recommended for grease application.

2.2.   Prepare the silicone encapsulant to fill the chamber. Mix a 10:1 ratio (by weight) of base to curing agent. Mix thoroughly but gently, using a micropipette tip to create minimal bubbles.

2.2.1. Pour the silicone encapsulant onto the affixed coverslip so that it is level with the surface of the chamber. Approximately 3 g of encapsulant will fill the chamber.

2.2.2. Carefully tap the chamber against a flat surface while keeping it horizontal, or use a micropipette tip (under a stereomicroscope) to remove or pull bubbles to the edge of the chamber.

2.2.3. Place the chamber in a laboratory oven overnight at 60-70 °C. Place the chamber inside of a ventilated box to ensure that hot air is not directly blowing on the encapsulant to avoid creating ripples.

2.3.   Use fine forceps and tungsten wire to fashion the pins used to immobilize larvae through the head and tail (**Figure 2B1**) on the hardened encapsulant.

2.3.1. To make head pins, hold a piece of 0.035 mm tungsten wire in one hand under a stereomicroscope. Using fine forceps in the other hand, bend the wire 1 mm up from the end at 90°. Exchange the forceps for fine scissors and cut 1 mm after the bend to create the pin.

2.3.2. Repeat step 2.3.1 using a 0.025 mm wire to make tail pins, but leave 0.5 mm of wire on either side of the bend. Use forceps to insert the pins into the hardened encapsulant on the chamber (for storage).

3. Preparation of Needles for Paralysis and Stimulation

220   3.1.   Prepare heart injection needles using glass capillaries with a filament. Pull needles to an
221   inner tip diameter of 1-3 µm (**Figure 2C**).

222

223   3.2.   Prepare fluid-jet needles using glass capillaries without a filament. Pull needles with a
224   thin, long tip that can be broken to the correct tip diameter.

225

226   3.2.1. Break off the thin, long tip of the fluid-jet needle by rubbing it perpendicularly against
227   another fluid-jet needle or a ceramic tile just above where the needle tip can be bent to create
228   an inner tip diameter of 30-50 µm [**Figure 2C** (middle image) and **Figure 3A2**]. Ensure that the
229   break is even across the tip (**Figure 2C**, middle image) and not jagged or too large (**Figure 2C**, right
230   image) to guarantee even and accurate fluid flow during hair-cell stimulation.

231

232   Note: A needle polisher can be used to fix jagged breaks.

233

234   **4. Pinning and Immobilizing Larva to Imaging Chamber**

235

236   4.1.   Bathe a Tg(myo6b:GCaMP6s-caax) larva in approximately 1 mL of E3 buffer containing
237   0.04% MS-222 for 1-2 min on the silicone encapsulant surface of the imaging chamber until the
238   larva becomes immobile or unresponsive to touch.

239

240   4.1.1. Under a stereomicroscope, position the larva at the center of the perfusion chamber so
241   it lies flat on its side against the silicone encapsulant.

242

243   Note: For consistency, always mount larvae on the same side (*e.g.*, right side down, left side up)
244   (**Figure 2B1**).

245

246   4.2.   Using fine forceps, bring a 0.035 mm head pin down perpendicular to the larva and
247   chamber. Insert the head pin between the eye and otic vesicle and down into the encapsulant
248   (**Figures 2B1** and **2B2**). Use a second set of forceps to stabilize the larva along its dorsal or ventral
249   side while pinning. Ensure that the horizontal part of the pin contacts the larva and does not
250   press all the way into the encapsulant. Angle the pin ventrally (**Figure 2B1**) or pointing slightly
251   toward the anterior of the fish to avoid interfering with subsequent heart injection and hair-cell
252   imaging.

253

254   4.2.1. Using the forceps, insert a 0.025 mm tail pin into the notochord as close as possible to the
255   end of the tail (**Figure 2B1**).

256

257   Note: Be careful to avoid stretching the larva. Pin the larva flat. Eyes should be superimposed
258   (**Figure 2B1**). This is very important for ease of heart injection (**Figure 2B2-B2'**, step 5), facilitating
259   a desirable imaging plane (**Figure 1B1-B2''**, steps 8 and 9), and quantifying the intensity of the
260   fluid-jet stimulus (**Figure 3A3**, step 7).

261

262   **5. Injection of α-Bungarotoxin into the Heart Cavity to Paralyze Larva**

263

264   Note: Wear gloves when handling α-bungarotoxin.
265
266   5.1.   Centrifuge the α-bungarotoxin aliquot briefly prior to use to prevent clogging of the heart
267   injection needle.
268
269   5.1.1. Backfill 3 µL of α-bungarotoxin solution into a heart injection needle using a gel loading
270   pipette tip. Load the solution evenly to the tip with no bubbles.
271
272   5.1.2. Insert the heart injection needle into a pipette holder attached to a manual
273   micromanipulator. Under a stereomicroscope, position the needle so it is aligned perpendicular
274   to the A-P axis of the pinned and anesthetized larvae, pointing down at an angle of ~30°.
275
276   5.1.3. Connect the pipette holder to the pressure injector. Apply the following suggested
277   settings: Pinjection = 100 hPa, tinjection = 0.5 s, and Pcompensation = 5 hPa. Inject a bolus into
278   the solution to test whether the needle tip is patent.
279
280   5.1.4. Look for a small puff of the red solution (from phenol red) to leave the tip of the needle.
281   If no red color is seen, very gently scrape the needle tip against the edge of a pin and try again
282   until the needle is patent. Alternatively, pull a needle with a larger tip opening.
283
284   5.2.   Advance the needle toward the heart until it touches the skin outside of the heart (**Figure
285   2B2**). Press the needle into the larva and look for indentation of the pigment cell on the skin in
286   front of the heart to ensure that needle is positioned in the correct plane relative to the larva
287   (**Figure 2B2'**).
288
289   5.2.1. Advance the needle further until it pierces the skin and enters the heart cavity. Pull the
290   needle back slightly. Inject a bolus of α-bungarotoxin into the heart cavity. Look for inflation of
291   the heart cavity or for red dye entering the cavity.
292
293   5.3.   Gently rinse the larva 3 times with 1 mL of NB to remove residual MS-222. Never remove
294   all of the fluid. Maintain larva in approximately 1 mL of NB on the perfusion chamber.
295
296   Note: Ensure that larval heart beat and blood flow remain robust after pinning and heart injection
297   and throughout the entire imaging experiment.
298
299   **6. Preparation of Microscope and Fluid-jet Setup**
300
301   6.1.   Assemble an upright confocal microscope using the components described in the **Table
302   of Materials**: a confocal microscope with a 488 nm laser and appropriate filters, microscope
303   software to control and coordinate imaging and stimulation, 10X air objective, 60X water
304   objective, piezo-Z objective scanner (for z-stacks), high-speed camera, circular chamber adaptor,
305   motorized stage, and stage insert adaptor. Refer to Zhang *et al.*[29] for additional options and
306   guidance on microscope setups.
307

308   6.2.   Assemble the fluid jet made up of 3 main components: a vacuum and pressure pump,
309   high-speed pressure clamp, and head stage (also described in the **Table of Materials**). Use the
310   high-speed pressure clamp to control the timing and duration of pressure or vacuum discharge
311   out of the heads stage and into the fluid-jet pipette.
312
313   6.2.1. Connect the output of the head stage to the fluid-jet pipette holder *via* thick-walled
314   silicone tubing.
315
316   **7.   Alignment of Larva and Fluid-Jet**
317
318   Note: There are 3 planes of interest within each neuromast: (1) the tips of the hair bundles (**Figure
319   3A3**: the kinocilia, used to measure stimulus intensity); (2) the hair-bundle MET plane (**Figure
320   1B1-B1'**: the base of the apical hair bundles where MET-channel-dependent calcium signals are
321   detected); and (3) the synaptic plane (**Figure 1B2-B2'**: where presynaptic calcium signals are
322   detected at the base of the hair cell). These planes are outlined in **Figure 1A**.
323
324   7.1.   Backfill 10 µL of NB into a properly broken fluid-jet needle (from step 3.2) using a gel
325   loading tip. Load the solution evenly to the tip with no bubbles. Insert the needle into the pipette
326   holder attached to the motorized micromanipulator.
327
328   7.2.   Place the perfusion chamber into a circular chamber adapter on the microscope stage.
329
330   Note: For consistency, always position the larva in the same orientation (*e.g.*, the chamber
331   containing the larva with its posterior toward fluid jet and ventral side facing toward the
332   experimenter).
333
334   7.2.1. Move the motorized stage so that the larva is in the center of the field of view. Turn the
335   circular chamber adaptor so that the A-P axis of the larva is roughly aligned with the trajectory
336   of the fluid-jet needle.
337
338   7.2.2. Using transmitted light and differential interference contrast (DIC), bring the larva into
339   focus and center it under the 10X objective. Raise the 10X objective.
340
341   7.3.   Using the motorized micromanipulator, bring the fluid-jet needle down into the center of
342   the field of view so it is illuminated by the transmitted light and barely touching the NB solution.
343
344   7.3.1. Lower the 10X objective. Focus on the larva to confirm its location. Focus up to find the
345   fluid-jet needle. Move the fluid-jet needle with the micromanipulator in the x- and y-axes until it
346   is in a position parallel to the dorsal side of the fish.
347
348   7.3.2. Focus back on the larva. Bring the needle down in the z-axis. Position the needle along
349   the dorsal side of the fish and ~1 mm away from the body (**Figure 3A1**).
350

351 7.3.3. Carefully move the circular chamber adaptor (if necessary) to ensure that the fluid-jet
352 needle is aligned along the A-P midline of the larva (**Figure 3A1**).

354 7.3.4. Move the motorized stage to place the neuromast of interest in the center of the field of
355 view. Keep the fluid-jet needle tip along the dorsal side of the fish. Do not touch the tip of the
356 fluid-jet needle to the larva or the chamber surface.

358 7.4. Switch to the 60X water objective. Ensure that the objective is immersed in the NB
359 solution. Use the fine focus to locate a neuromast using transmitted light and DIC optics.

361 Note: This setup is designed to stimulate neuromasts along the primary posterior lateral line. Hair
362 cells within these neuromasts respond to either anterior or posterior directed fluid flow. See
363 Chou *et al.*[31] for an accurate map of neuromast fluid sensitivity within the lateral-line system.

365 7.4.1. Position the fluid-jet needle with the micromanipulator so that it is 100 µm from the outer
366 edge of the neuromast (**Figure 3A2**).

368 Note: Choose neuromasts that offer clear top-down views (**Figures 1B1'-B2'** and **Figure 3A3**)
369 rather than side-angled views (**Figure 1C1-C2**). A clear top-down view allows for simultaneous
370 imaging of all apical hair bundles in a single optical plane or imaging of synaptic areas in fewer
371 optical planes (**Figure 3A3**).

373 7.4.2. Focus up to the tips of the apical hair-bundles (kinocilia) (**Figure 1A**, **Figures 3A2** and **3A3**).
374 The bottom of the fluid-jet needle should be in focus in this plane.

376 7.5. Set the high-speed pressure clamp from the manual to external mode to receive input
377 from the imaging software.

379 7.5.1. Zero the high-speed pressure clamp by pressing the "zero" button. Use the set-point knob
380 to set the resting pressure slightly positive (~2 mmHg). Confirm the resting output of the high-
381 speed pressure clamp using a PSI manometer attached to the head stage output.

383 Note: Set a slightly positive pressure at rest to avoid the gradual uptake of fluid into the fluid-jet
384 needle over time. If fluid enters the tubing connected to the fluid-jet and reaches the head stage,
385 it can damage the equipment.

387 7.5.2. Determine the pressure needed to stimulate the hair bundles. Use a 0.125 and 0.25 V
388 input (6.25 and 12.5 mmHg) for 200-500 ms to apply a test stimulus (**Figure 3A3-A3''**).

390 Note: The high-speed pressure clamp converts a voltage input (from software or other devices
391 that connect to the BNC port on the high-speed pressure clamp command port) into pressure
392 that is discharged from the head stage, and ultimately, the fluid-jet needle (1.0 V = 50 mmHg,
393 while -1.0 V = -50 mmHg). In this configuration (see step 7.2) positive pressure (push) deflects

394 hair bundles towards the anterior, and negative pressure (pull) deflects hair bundles towards the
395 posterior.
396
397 <mark>7.5.3.   Using transmitted light and DIC optics along with a scale bar, measure the distance of</mark>
398 <mark>deflection by the 6.25 and 12.5 mmHg stimuli of the tips of the hair bundles, the kinocilia (**Figure**</mark>
399 <mark>**1A** and **Figures 3A3-3''**). Choose a pressure that moves the bundles (as 1 cohesive unit) a distance</mark>
400 <mark>of approximately 5 μm (**Figure 3A3''**). Ensure that the tips of the kinocilia remain in focus the</mark>
401 <mark>entire time.</mark>
402
403 <mark>7.5.4.   Move the fluid-jet ± 25 μm along the A-P axis of the larva to find a distance and pressure</mark>
404 <mark>that deflects the tips of kinocilia 5 μm.</mark>
405
406 Note: Using GCaMP6s in larvae 3-7 dpf, a 5 μm deflection should achieve near saturating
407 GCaMP6s calcium signals and should not damage apical hair-bundle structures (**Figure 3A3''**).
408 Smaller displacement distances can be used to deliver non-saturating stimuli (**Figure 3A3'**).
409 Displacement distances > 10 μm are hard to estimate (**Figure 3A3'''**) and can be damaging over
410 time. Signal saturation is dependent on age of the neuromast (and kinocilial height) as well as the
411 indicator used. Check the patency of the fluid-jet needle in each direction (pressure/push and
412 vacuum/pull) periodically during imaging. Fluid-jet needles clog easily and lose vacuum patency,
413 but they maintain residual pressure patency. Use DIC optics and a short test stimulus in each
414 direction to check for fluid-jet patency.
415
416 <mark>7.5.5.   Focus the sample into the plane of interest (*e.g.*, the base of the apical hair bundles or</mark>
417 <mark>the base of the hair cell in the synaptic plane; **Figure 1B1-B2'**).</mark>
418
419 <mark>8.   **Imaging Acquisition Procedure Option 1: Single-plane Acquisition**</mark>
420
421 Note: All imaging outlined in this protocol is performed at RT.
422
423 8.1.   Set imaging software to acquire a streaming or continuous 80-frame acquisition with a
424 capture every 100 ms to achieve a frame rate of 10 Hz.
425
426 8.2.   Set gain, aperture, and laser power to optimize signal detection, but avoid saturation,
427 photobleaching, and noise. Example settings for an Opterra/SFC are as follows: 488 nm laser
428 power: 50 (hair-bundle MET plane), 75 (synaptic plane); 35 μm slit; gain = 2.7; EM gain = 3900.
429
430 Note: Apply 2 X binning if signals are too weak or noisy or have excessive photobleaching. 2 X
431 binning will enhance signal detection at the cost of spatial resolution.
432
433 <mark>8.3.   Select a stimulus to deliver during the 80-frame (8 s) acquisition after frame 30, at 3 s.</mark>
434
435 Note: Some example stimuli are as follows: 200 ms (+ or - 0.25 V) up to 2 s (+ or - 0.25 V) step in
436 the anterior or posterior direction to identify the directional sensitivity of each hair cell; 2 s, 5 Hz
437 square wave (0.25 V for 200 ms, -0.25 V for 200 ms, repeated 5 times) to stimulate all hair cells

438 simultaneously. A positive pressure (anterior stimulus) will activate half of the hair cells. A
439 negative pressure (posterior stimulus) will activate the other half of the hair cells. Be sure the
440 stimulus software or device returns the pressure clamp back to 0 V after the stimulus is finished.
441
442 8.4.   Measure mechanosensitive calcium responses. Focus on the base of the apical hair
443 bundles (**Figures 1A** and **1B1-B1'**) and start image acquisition.
444
445 Note: If the neuromast is viewed clearly from the top down (**Figure 1B1-B1'**), all apical hair
446 bundles can be imaged simultaneously in a single plane.
447
448 8.5.   Measure presynaptic calcium responses. Focus to the base of the hair cells (**Figures 1A**
449 and **1B2-B2'**) and start image acquisition.
450
451 Note: If the neuromast is viewed clearly from the top down (**Figure 1B2-B2'**), the presynaptic
452 imaging planes of all hair cells can be acquired in 2-3 planes set 2 µm apart. *Tg[myo6b:ribeye-*
453 *mcherry]* transgenic fish can be used to identify and locate presynaptic ribbons and sites of
454 calcium entry[29].
455
456 **9.   Imaging Acquisition Procedure Option 2: Multi-plane Acquisition**
457
458 9.1.   Tune the piezo-Z attached to the 60X objective for fast acquisitions (12-18 ms). Ensure
459 that max-speed settings are selected.
460
461 9.2.   Create a Z-stack acquisition using a piezo-Z. Acquire the hair-bundle MET activity in 5
462 planes with step size of 0.5 µm. Acquire the presynaptic signals in 5 planes with step size of 1 µm.
463
464 9.3.   Set the frame rate to 10 Hz. Each frame will be captured every 20 ms and each Z-stack
465 every 100 ms.
466
467 9.4.   Set up the acquisition for 400 frames or 80 Z-stacks at 10 Hz for an 8 s streaming
468 acquisition.
469
470 9.5.   Set laser power, aperture, and gain to optimize signal detection, but avoid saturation,
471 photobleaching, and noise. Example settings for an Opterra/SFC system are as follows: 488 nm
472 laser power: 75 (hair-bundle MET plane), 125 (synaptic plane); 35 µm slit; gain = 2.7; EM gain =
473 3900.
474
475 Note: Apply 2 X binning if signals are too weak, noisy, or have excessive photobleaching. 2 X
476 binning will enhance signal detection at the cost of spatial resolution.
477
478 9.6.   Select a stimulus to deliver during the acquisition starting at frame 150, after 3 s.
479
480 9.7.   Continue the protocol as described above for single plane acquisition, but center the Z-
481 stack in the apical or basal planes (steps 8.4 and 8.5).

482

10. Control: Pharmacological Block of All Evoked Calcium Signals

Note: BAPTA (1,2-bis(o-aminophenoxy)ethane-N,N,N',N'-tetraacetic acid) treatment is a critical control when first establishing this protocol.

10.1.   After completing steps 8 or 9, replace the NB with 1 mL of NB containing 5 mM BAPTA to cleave the tip links required to gate apical MET channels located in hair bundles.

10.2.   Incubate for 10-20 min at RT.

10.3.   Wash off BAPTA 3 times with 1 mL of NB.

10.4.   Repeat step 8 or 9. After BAPTA treatment, there should be no change in GCaMP6s fluorescence in response to fluid-jet stimulation in either the apical hair bundles or synaptic plane. If changes in GCaMP6s fluorescence persist, these are not true calcium signals and may be motion artifacts.

11. Control: Pharmacological Block of Presynaptic Calcium Signals (Optional)

11.1.   After completing steps 8 or 9, replace the NB with NB containing 10 µM isradipine with 0.1% dimethyl sulfoxide (DMSO) to block the L-type calcium channels at the hair-cell presynapse.

11.2.   Incubate for 10 min at RT.

11.3.   Without performing a wash, repeat step 8 or 9. After treatment, there should still be GCaMP6s fluorescence changes in response to fluid-jet stimulation in apical hair-bundles but not the synaptic plane. If changes in GCaMP6s fluorescence persist in the synaptic plane, these are not true calcium signals and may be motion artifacts.

12. Image Processing and Graphical Representation of Data

Note: Use Fiji (steps 12.1-12.1.5) and a graphing program (steps 12.2-12.2.3) for step 12. StackReg, TurboReg (step 12.1.3), Time Series Analyzer V3 (steps 12.1.4-12.1.6), and Fiji plugins are also required (see **Table of Materials**).

12.1.   Open an image sequence in Fiji, either a single-plane time series (80-frame single plane) or Z-stack time series (400-frame multi plane). Click on "File," select "Import" from the drop-down menu, and click on "Image Sequence."

12.1.1. For a Z-stack times series, Z-project each time point (5 planes per timepoint) to create an 80-frame image sequence. Click on "Image," select "Stacks" from the drop-down menu, select "Tools" from the drop-down menu, and click on "Grouped Z-project." Select "Average Intensity" as the Projection method, and enter "5" for "Group size".

526
527   Note: Each plane within the Z-stack can be analyzed separately for additional spatial information.
528
529   12.1.2. Remove the first 1 s (10 frames) from the 8 s (80 frames) of image acquisition. Click on
530   "Image," select "Stacks" from the drop-down menu, select "Tools" from the drop-down menu,
531   and click on "Make Substack." Enter "11-80" for "Slices".
532
533   Note: This substack will be referred to as *stk1*.
534
535   12.1.3. Register the image sequence (*stk1*) using the StackReg plugin[32]. Click on "Plugins," select
536   "StackReg", and select "Translation" as the method of registration for the 70-frame time series.
537
538   Note: This registered substack will be referred to as *stk2*.
539
540   12.1.4. Use the Times Series Analyzer V3 plugin to extract the GCaMP6 intensity (F)
541   measurements. Place a region of interest (ROI) on apical hair bundles or presynaptic sites in *stk2*.
542   Refer to the ImageJ website (see **Table of Materials** for the link) for instructions on how to use
543   Time Series Analyzer V3.
544
545   Note: Use a circular 1-2 µm ROI for apical hair bundles and a circular 3-5 µm ROI for the synaptic
546   plane (**Figures 4A1** and **4A2**).
547
548   12.1.5. Select the measurement parameters. Click on "Analyze," select "Set Measurement," and
549   ensure that only "Mean gray value" is selected.
550
551   12.1.6. In the ROI manager, select all ROIs and use the multi-measure function to generate (F)
552   intensity values for each ROI in the time series. Within ROI Manager, click "More >> ," and select
553   "Multi Measure" from the drop-down menu.
554
555   12.2.   Plot (F) values. Paste the values (F) from the "Multi Measure" Results into a graphing
556   program to create an X-Y graph (**Figures 4A1'** and **4A2'**).
557
558   Note: Create (X) values manually or use the time stamp from the metadata.
559
560   12.2.1. Quantify the baseline (F_o) for each ROI by averaging the (F) values in the graphing program
561   from the pre-stimulus frames 1-20.
562
563   12.2.2. For each ROI, subtract the (F_o) from the (F) values at each timepoint to create ΔF (F-F_o)
564   values. Replot, if desired.
565
566   12.2.3. Calculate and plot $\Delta F/F_o$. For each ROI, divide the ΔF measurement by (F_o) and replot
567   (**Figures 4A1''** and **4A2''**).
568
569   **13. Image Processing and Heat Map Representation of Spatio-temporal Calcium Signals**

570

571 Note: Previous work to create spatial heat map representation of calcium signals in zebrafish
572 lateral-line hair cells have used custom software written in in Matlab[5,28]. This analysis has been
573 adapted for the open source analysis software Fiji[33]. Use Fiji for all steps outlined below. StackReg
574 and TurboReg Fiji plugins are also required (see **Table of Materials**).

575

576 13.1.   Perform steps 12.1-12.1.3 for each Z-stack or single plane time series to create the
577 registered substack referred to as *stk2*.

578

579 13.2.   Use *stk2* to create a baseline image. Click on "Image," select "Stacks" from the drop-down
580 menu, and select "Z Project". Select "Average Intensity" for "Projection type", and enter "1" for
581 "Start slice" and "20" for "Stop slice".

582

583 Note: This Z-projection will be referred to as *baselineIMG*.

584

585 13.2.1. Temporally bin the 70-frame (F) image sequence (*stk2*) into 14 0.5-s bins. Click on
586 "Image," select "Stacks" from the drop-down menu, select "Tools" from the drop-down menu,
587 and click on "Grouped Z Project". Select "Average Intensity" as the "Projection method," and
588 enter 5 for "Group size."

589

590 Note: This grouped Z-projection will be referred to as *stk2bin* and F in **Figure 5**.

591

592 13.2.2. Subtract the pixel value of baseline (*baselineIMG*) from the binned (F) image sequence
593 (*stk2bin*) to create a ΔF image sequence. Click on "Process" and select "Image Calculator" from
594 the drop-down menu. Select *stk2bin* as "Image1" and *baselineIMG* as "Image2." Select "Subtract"
595 for "Operation."

596

597 Note: This baseline-subtracted Z-projection is referred to as *stk2binBL* and F-BL = ΔF in **Figure 5**.

598

599 13.3.   Choose a lookup table (LUT) of choice to display ΔF image sequence (*stk2binBL*). Click on
600 "Image," select "Lookup Tables" from the drop-down menu, and click on a LUT of choice.

601

602 Note: "Red Hot" is the LUT used in **Figure 5**. This baseline-subtracted Z-projection with LUT is
603 referred to as *stk2binBL-LUT* and ΔF LUT in **Figure 5**.

604

605 13.3.1. Set the minimum (min) and maximum (max) brightness values for *stk2binBL-LUT*. Click on
606 "Image," select "Adjust," and click on "Brightness/Contrast". Set the min value to remove
607 background noise from *stk2binBL-LUT*. Set the max values to retain signals of interest but avoid
608 signal saturation [*e.g.*, 200 to 1600 (12-bit image intensity range = 0 to 4095)].

609

610 Note: Use the same min and max values when making visual comparisons or representations. A
611 ΔF calibration LUT bar can be generated in Fiji for each LUT image sequence (*e.g.*, *stk2binBL-LUT*).
612 Click on "Analyze," select "Tools," and click on "Calibration Bar". Unclick "Overlay" to generate a
613 separate, individual image with the LUT calibration bar for reference.

614

615   13.3.2. Convert both the ΔF (*stk2binBL-LUT*) with the desired LUT and the temporally binned (F)
616   image (*stk2bin*) sequences to RGB. Click on "Image," select "Type," and click on "RGB Color."

617

618   Note: The RGB-converted Z-projections will be referred to as *stk2binBL-LUT-RGB* and *stk2bin-*
619   *RGB*, respectively.

620

621   13.4.   Overlay the ΔF LUT images (*stk2binBL-LUT-RGB*) onto binned (F) images (*stk2bin-RGB*).
622   Click on "Process" and then "Image Calculator". Select *stk2bin-RGB* as Image1 and *stk2binBL-LUT-*
623   *RGB* as Image2. Select "Transparent-zero" for "Operation".

624

625   Note: If there is too much noise or background in the ΔF LUT overlay, repeat step 13.3 to increase
626   the min value. If there is saturation, repeat step 13.3 and increase the max value.

627

628   **14.   Image Processing and Spatio-temporal Heat Map Representation Using a Fiji Macro**

629

630   Note: The following section refers to a Fiji macro called LUToverlay based on step 13 that will
631   automatically create spatial heat map representation of GCaMP6s signals. This analysis requires
632   the open source analysis software Fiji[33] and the StackReg and TurboReg Fiji plugins (see **Table of**
633   **Materials**).

634

635   14.1.   Download the Fiji LUT overlay macro (LUToverlay.ijm) accompanying this protocol (see
636   **Supplemental Coding File**).

637

638   14.2.   Open either a multi-plane time series or single-plane time series (see step 12.1).

639

640   14.3.   Click on "Plugins," select "Macros," click on "Run," and select the LUToverlay macro. A
641   dialog box will appear with the text, "Tell me about your image acquisition".

642

643   Note: For the dialog box, the numbers present are suggested values and can be changed
644   according to the setup used by the experimenter. The values listed in the box and below are set
645   for a multi-plane time series with 400 images and 5 planes per timepoint (step 9).

646

647   14.4.   After "Number of planes per timepoint", enter the number of planes per timepoint (*e.g.*,
648   for step 12.1.1 using a multi-plane 400 time series with 5 planes per timepoint, enter "5"). For a
649   single plane acquisition (*e.g.*, step 8) enter "1".

650

651   Note: In the remaining dialog boxes, for a multi-plane time series, "Timepoints" refers to the
652   number images in the projected Z-stack (*e.g.*, for step 12.1.1 this is 80 timepoints).

653

654   14.4.1. Use the "Define the range to analyze" option to remove the first 1 s of the image sequence
655   (*e.g.*, for step 12.1.2 select "11-80" to remove the first 10 frames and first 1 s).

656

657   14.4.2. After "Define timepoints in baseline", enter the number of images to be used to create
658   the baseline image [*e.g.*, for step 13.2., enter "20" to use the pre-stimulus images (11-30)].

660   14.4.3. After "Timepoints per temporal bin" enter the number of images to bin for the overlay.
661   (*e.g.*, for step 13.2.2. select "5" to create 14 0.5-s bins).

663   14.4.4. After "Min intensity" and "Max intensity" enter the minimum and maximum brightness
664   values that will remove background noise (minimum) and retain signals of interest while avoiding
665   saturation (maximum).

667   14.4.5. After "Choose a lookup table", select the LUT desired for the overlay. Click "OK".

669   Note: The macro will finish analyzing the images according to the instructions presented in step
670   13. The images generated by the macro will also be named according to the instructions in step
671   13.

673   14.5.   Close all analysis windows before processing a new image sequence.

675   **REPRESENTATIVE RESULTS:**
676   After myo6b:GCaMP6s-caax transgenic fish are properly immobilized and the fluid-jet stimulus is
677   delivered to lateral-line hair cells, robust calcium signals can be visualized and measured (**Figures
678   4** and **5**, taken at 2 X binning). During fluid-jet stimulation, calcium signals can either be measured
679   in the apical hair bundles, where MET channels open in response to stimuli, or at the base of hair
680   cells, where presynaptic $Ca_v1.3$ calcium channels trigger neurotransmission. A representative
681   example of calcium responses in these regions with an individual neuromast are shown in **Figure
682   4A1-A2''**. In this example, a 2-s 5 Hz fluid-jet stimulus was delivered to activate all hair cells within
683   the representative neuromast. During the stimulus, robust calcium signals can be detected in hair
684   bundles (**Figure 4A1-A1''**, responses from 8 hair bundles are shown). In this system, nearly all
685   mature hair cells display this apical influx of calcium[5]. In contrast, within the same neuromast,
686   there are detectable calcium signals in the basal, synaptic plane in only a subset (~30%) of hair
687   cells (**Figure 4A2-A2''**, 4 cells with presynaptic responses are shown)[5]. The 4 green ROIs show
688   cells with no significant presynaptic calcium signals (**Figure 4A2-A2''**) despite robust apical
689   calcium signals (**Figure 4A1-A1''**). In this representative example (**Figure 4A1-A2''**), colored ROIs
690   match up hair bundles in the apical MET plane (**Figure 4A1**) with their cell bodies in the basal
691   synaptic plane (**Figure 4A2**). This example highlights how both MET dependent- and presynaptic-
692   calcium signals can be measured within individual hair cells and among populations of hair cells.

694   The calcium signals in both the hair bundles and at the presynapse can be plotted graphically as
695   either raw (F) GCaMP6s intensity or $\Delta F/F_o$ GCaMP6s intensity (see step 12, **Figures 4A1'-A1''** and
696   **4A2'-A2''**). The (F) GaMP6s graphs highlight that the baseline fluorescence intensity for each cell
697   can differ (**Figures 4A1'** and **4A2'**). In the $\Delta F/F_o$ GCaMP6s graphs, each cell is normalized to its
698   baseline value and the relative intensity change from baseline is plotted (**Figures 4A1''** and **4A2''**).
699   In both the (F) and $\Delta F/F_o$ GCaMP6s plots, the calcium signals in both the apical hair bundle and
700   basal presynaptic plane initiate with the onset of the stimulus (gray box) and decline

701 exponentially after the stimulus ends. During the stimulus, calcium signals in hair bundles rise
702 rapidly and saturate if the strength of the deflection does not change (**Figure 4A1-A1''**). In
703 contrast, within the subset of hair cells with detectable calcium signals in the synaptic plane, the
704 calcium signals increase more gradually and are less prone to saturation (**Figure 4A2-A2''**). In hair
705 cells without presynaptic calcium signals (green ROIs), the calcium signals remain near baseline.
706
707 In addition to these graphical representations (**Figure 4**), calcium signals can be visualized
708 spatially within the entire neuromast during the time course of the recording. An example of a
709 spatiotemporal representation is shown in **Figure 5** for presynaptic GCaMP6s signals in the basal
710 plane of a neuromast. In **Figure 5**, the main steps to process an image sequence for spatial
711 visualization are outlined as described in step 13. First, the raw (F) GCaMP6s images are
712 temporally binned [**Figure 5**: row 1 (5 of the 14 bins are shown); step 13.2.1]. Then, the baseline
713 image, calculated from pre-stimulus frames (step 13.2), is subtracted from the (F) GCaMP6s
714 fluorescence signals to obtain ΔF images (**Figure 5**: row 2; step 13.2.2). Next, the ΔF grayscale
715 images are converted to a color LUT (**Figure 5**: row 3, Red Hot LUT; step 13.3). Finally, the ΔF
716 images with the LUT conversion are overlaid onto the temporally binned (F) images (**Figure 5**,
717 first row) to reveal the spatiotemporal signals within the neuromast during stimulation (**Figure 5**:
718 row 4; step 13.4). The heat maps of ΔF GCaMP6s signals provide both valuable spatial and
719 temporal information that is not easy to parse out from single ROIs and the graphs used in **Figure
720 4**. Heat maps can help visualize critical spatiotemporal information, including subcellular
721 information regarding the onset and duration of calcium signals within each hair cell as well as
722 the timing and intensity differences among hair cells within the entire neuromast.
723
724 It is important to verify that the graphs and spatial heat maps represent true calcium signals and
725 are not artifacts due to motion. In this protocol, motion artifacts can be the result of excessive
726 drift or movement of the larva or motion due to fluid-jet stimulation. All of these artifacts are
727 challenging to completely eliminate in this *in vivo* preparation. While registration of image
728 sequences (step 12.1.3) can correct for the majority of movement in x- and y-axes, image
729 sequences with excessive movement in the z-axis must be identified and removed from analyses.
730 Motion artifacts are easiest to identify by graphing the calcium signals. Examples of GCaMP6s
731 intensity changes that are artifacts and are not true GCaMP6s signals can be observed at the apex
732 (**Figure 4B1'-B1''**) and base (**Figure 4C1'-C1''**) of hair cells.
733
734 In the apical hair bundles, motion artifacts are common when the fluid-jet stimulus is too strong
735 (**Figure 3A3'''**). During these excessively strong stimuli, the apical hair-bundle plane can move
736 out of focus during fluid-jet stimulation then return to the original focal plane after the stimulus
737 terminates (**Figure 4B1'-B''**). This makes it difficult to accurately measure apical MET-dependent
738 calcium signals. An example of hair-bundle motion artifacts can be seen in **Figure 4B1'-B1''**. Here,
739 the graphs show a decrease in GCaMP6s signals during the stimulus (gray box) when the hair
740 bundles are out-of-focus. After the stimulus ends, the GCaMP6s signals rapidly increase as the
741 hair bundles return to their original position and come back into focus. This contrasts with the
742 example in **Figure 4A1'-A1''** in which the apical calcium signals increase at the onset of the
743 stimulus and decrease when the stimulus ends.
744

745 While movement due to excessive fluid-jet stimuli can also move the synaptic plane out of focus,
746 this type of motion artifact is less common in this plane. Instead, changes in focus in the Z-axis
747 due to movement or drift of the larva are the most common causes of motion artifacts. Larval
748 motion or drift can affect GCaMP6s measurements at both the apex and base of hair cells. An
749 example of larval motion that increases GCaMP6s in the basal, synaptic plane during the stimulus
750 is shown in **Figure 4C'-C''**. Motion artifacts (**Figure 4C1'-C1''**) can be distinguished from true
751 presynaptic signals (**Figure 4A2'-A2''**) by examining the time course of the GCaMP6s signals.
752 Rather than increasing and decreasing exponentially with the stimulus (**Figure 4A2'-A2''**), the
753 motion-induced increases in GCaMP6s signal have a square shape and rise and fall abruptly with
754 the onset and offset of the stimulus, respectively (**Figure 4C1'-C1''**).

756 In addition to careful examination of the time course of GCaMP6s signals, control experiments
757 using pharmacology can be used to differentiate true GCaMP6s signals from motion artifacts. For
758 example, BAPTA (step 10) can be applied to cleave the tip-links that are required for MET-channel
759 function in hair bundles. BAPTA should eliminate both fluid-jet-evoked apical MET-channel-
760 dependent calcium influx as well as the subsequent basal, presynaptic calcium influx through
761 $Ca_v1.3$ channels. In the representative example of true stimulus-evoked calcium signals (**Figure
762 4A1-A2''**) during fluid-jet stimulation, all changes in GCaMP6s fluorescence in both the apical and
763 basal planes would be eliminated after BAPTA treatment. In contrast, changes in GCaMP6s
764 fluorescence due to motion such as those shown in **Figures 4B1'-B1''** and **4C1'-C1''** would not be
765 eliminated by BAPTA treatment.

767 In addition to using BAPTA to eliminate all stimulus-evoked GCaMP6s signals, isradipine can be
768 applied (step 11) to specifically block $Ca_v1.3$-dependent calcium influx in the basal synaptic plane
769 while leaving apical MET-channel-dependent calcium influx intact[5]. After application of
770 isradipine, in an individual neuromast with no motion artifacts, changes in GCaMP6s fluorescence
771 in apical hair bundles (**Figure 4A1'-A1''**) during fluid-jet stimulation would be unaltered, while all
772 synaptic GCaMP6s fluorescence changes at the base would be eliminated (**Figure 4A2'-A2''**). Any
773 change in GCaMP6s signal in the synaptic plane after isradipine application (*e.g.,* **Figure 4C1-C1''**)
774 would most likely correspond to motion artifacts.

776 **FIGURE LEGENDS:**
777 **Figure 1**: **Overview of a lateral-line neuromast and functional imaging planes. (A)** The diagram
778 to the left depicts a side-view of a neuromast with four hair-cell bodies (black) contacting
779 postsynaptic afferent neurons (blue). Ribbons (green) tether vesicles at presynaptic active sites
780 within each cell. Apical to each cell body is a bundle of stereocilia (1 μm) that contain MET
781 channels. Each hair bundle has one kinocilium that transfers the mechanical force of water
782 motion to the base of the hair bundle. The diagram on the right depicts the same model in a top-
783 down view. In this top-down view, black is used to indicate the four cells depicted in the diagram
784 on the left, and gray is used to indicate other cells in the neuromast. Within this model and these
785 2 views, three important planes are highlighted: (1) the tips of the hair bundles (kinocilia) used
786 to quantify the magnitude of hair-bundle deflection, (2) the apical MET plane at the base of the
787 hair bundles where calcium enters the cell during stimulation, and (3) the synaptic plane at the
788 base of the cell where calcium enters near synaptic ribbons. **(B1-B1')** DIC and GCaMP6s top-down

789 images of MET plane at the base of the hair bundles, where mechanosensation-dependent
790 calcium signals can be recorded. **(B2-B2')** DIC and GCaMP6s top-down images from the same
791 neuromast as B1-B1', but at the base of the neuromast in the synaptic plane, where presynaptic
792 calcium signals can be detected. **(C1-C2)** Images of a neuromast expressing GCaMP6s where the
793 larvae is improperly mounted. In this example, the apical MET plane (C1) and synaptic plane (C2)
794 at the base of the cell are positioned at a suboptimal angle. This position does not allow for all
795 hair bundles to be imaged in a single plane, and many more imaging planes are needed to capture
796 activity at all synapses within this neuromast compared to B1-B2'. Images are of larvae at 5 dpf.
797 The scale bar in C2 corresponds to all images in B1-C2.
798
799 **Figure 2**: **Imaging chamber, zebrafish mounting and heart injection procedures, and needles.**
800 **(A)** Shown is an imaging chamber with a larva (outlined by a dashed rectangle) pinned to the
801 center atop the silicone encapsulant. **(B1)** Shown is a 5 dpf larva immobilized by two pins. A large
802 head pin is placed perpendicular to the body just posterior to the eye. The two eyes are
803 completely superimposed so the bottom eye is entirely obscured by the upper eye. A small tail
804 pin intersects the notochord in the tail. The larva is flat and not twisted. **(B2)** To paralyze larva, a
805 heart injection needle is oriented perpendicular to the body and brought adjacent to the heart.
806 The heart injection needle should contact the pigment cell in front of the heart. **(B2')** Depression
807 of the needle into the skin causes indentation of the pigment cell in front of the heart. **(C)** Needles
808 in order from left to right: example of a heart injection needle with an opening of approximately
809 3 μm; example of a good fluid-jet needle with an opening of approximately 50 μm; example of a
810 poorly broken fluid-jet needle that is large and jagged and will likely produce excessive and
811 irregular stimuli.
812
813 **Figure 3**: **Fluid-jet alignment, positioning, and stimulus calibration. (A1)** Shown is a larva
814 oriented with the head facing to the left and tail to the right, and a fluid-jet needle oriented
815 parallel to the A-P axis of the zebrafish body. This fluid-jet needle is aligned to stimulate the
816 neuromasts that respond to anterior (push/pressure) and posterior (pull/vacuum) directed fluid-
817 flow. **(A2)** Shown is a neuromast (outlined by dashed white line) and tips of apical hair bundles
818 (kinocilia) on the left side the panel and the fluid-jet needle on the right side of the panel. The
819 fluid-jet is positioned approximately 100 μm from the edge of the neuromast. **(A3-A3''')** The tips
820 of apical hair bundles (kinocilia) are deflected different distances by varying fluid-jet stimulus
821 pressures. The trajectory of a single kinocilial tip is shown for 1.5 μm (A3') and 5 μm (A3'')
822 deflection distances. The black circle indicates the resting position of the kinocilium. It is
823 important that kinocilia are not deflected too far, otherwise the stimulus intensity cannot be
824 reliably quantified and can become damaging (A3''').
825
826 **Figure 4**: **Apical MET and basal presynaptic GCaMP6s signals during fluid-jet stimulation in**
827 **lateral-line hair cells. (A1-A2'')** GCaMP6s intensity changes during fluid-jet stimulation within a
828 representative neuromast. The images on the left show the apical MET plane (A1) and basal
829 synaptic plane (A2) within the same neuromast. The ROIs color coded in A1 and A2 were used to
830 plot the time course of (F) and ΔF/F GCaMP6s intensity graphs to the right of each image. **(B1-**
831 **B1'')** Example of an apical MET image sequence with excess movement during fluid-jet
832 stimulation. The image on the left (B1) shows the ROIs used to plot the (F) and ΔF/F GCaMP6s

833   intensity graphs to the right. **(C1-C1'')** Example of an image sequence in the basal synaptic plane
834   that shows movement artifacts and GCaMP6s signal changes that are not true calcium signals.
835   The image on the left (C1) shows the ROIs used to plot the (F) and ΔF/F GCaMP6s intensity graphs
836   to the right. The gray box in each graph represents the duration of the fluid-jet stimulus during
837   each image sequence. A 2-s 5 Hz fluid-jet stimulus was used for the example in A1-A2'' and B1-
838   B1''. In C1-C1'', a 2 s anterior step stimulus was used. The Y axis for (F) GCaMP6s graphs depicts
839   arbitrary units (A.U.) obtained from Fiji image intensity measurements. All examples are from
840   larvae at 4-5 dpf. Scale bar = 5 μm for all images.
841
842   **Figure 5**: **Spatiotemporal visualization of presynaptic GCaMP6s signals during fluid-jet**
843   **stimulation.** The steps to visualize the spatiotemporal changes in GCaMP6s intensity within a
844   neuromast during stimulus are outlined. Time is represented from left to right according to the
845   time stamp at the top of the images. The top row shows 5 of the 14 temporal bins from a 70-
846   frame GCaMP6s (F) image sequence (step 13.2.1). In the second row, the baseline (step 13.2) has
847   been removed from each (F) GCaMP6s binned image to create ΔF images (step 13.2.2). In the
848   third row, ΔF images have been converted from grayscale (second row) to Red Hot LUT (step
849   13.3). The min and max of these LUT images are set according to the Red Hot LUT heat map of
850   relative ΔF intensity (A.U.) on the right (step 13.3.1). In the bottom row, the third row has been
851   overlaid onto the (F) images in the top row (step 13.4). The gray bar at the top of the figure
852   indicates the timing of the 2-s 5 Hz fluid-jet stimulus. The example is from a 5 dpf larvae. A legend
853   of the Red Hot LUT heat map of relative ΔF intensity (A.U.) is shown to the right. Scale bar = 5 μm
854   for all images.
855
856   **DISCUSSION:**
857   *In vivo* imaging in intact animals is inherently challenging. Several steps in this method are critical
858   to obtaining reliable *in vivo* calcium measurements from lateral-line hair cells. For example, it is
859   very important that the larva is pinned and paralyzed properly before imaging to minimize
860   movement during imaging. Excess movement during imaging can lead to changes in GCaMP6s
861   fluorescence that are not true signals and do not correspond to changes in calcium levels (*e.g.*,
862   **Figures 4B1'-B1''** and **4C1'-C1''**). Tail pins can be placed more anteriorly to help minimize
863   movement, though this may render more posterior neuromasts inaccessible. Furthermore, after
864   heart injection, head pins can be rotated so that the horizontal portion of the pin lies across the
865   yolk. In addition to altering the position of pins, it is also possible to use a brain-slice harp instead
866   of pins to immobilize larvae[34]. When placed over the larvae properly, a harp is an additional,
867   potentially less invasive method of immobilizing larvae. While significant movement can result
868   from inadequate pinning, failure to properly perform the heart injection to deliver α-
869   bungarotoxin and paralyze larvae can result in incomplete paralysis, movement, and ultimately
870   motion artifacts. Although commonly used anesthetics have been shown to affect the excitability
871   of zebrafish hair cells, recent work has shown that the anesthetic benzocaine does not interfere
872   with many aspects of hair-cell activity. Similarly, the more commonly used anesthetic MS-222
873   only interferes with certain aspects of hair-cell activity[15]. Therefore, due to the challenging nature
874   of α-bungarotoxin injection, benzocaine or MS-222 application may prove to be a useful
875   alternative method of paralysis to prevent movement in the larva during functional calcium
876   imaging.

877
878 In addition to the technical challenges involved in this protocol, even a perfectly mounted sample
879 is useless if the larva and hair cells are not healthy prior to and during each imaging experiment.
880 To ensure that larvae and hair cells are healthy, it is important that larvae are maintained in E3
881 buffer that is free of debris such as chorions (egg shells), waste, and microorganisms. Although
882 the superficial location of lateral-line hair cells is advantageous for imaging, this location makes
883 them more vulnerable to cellular damage when the E3 buffer is fouled. A clean, aqueous
884 environment is particularly important for young larvae (2-4 dpf) or mutants that cannot maintain
885 an upright swimming position and primarily lie on the bottom of the Petri dish. In these situations,
886 lateral-line hair cells and the protective cupula surrounding the hair bundles can easily become
887 compromised. Even when starting with healthy larvae and hair cells, throughout the course of
888 each experiment, it is critical to ensure that the larva has a heartbeat and rapid blood flow. If
889 blood flow slows or stops, the health of the hair cells can become compromised. In compromised
890 preparations involving unhealthy larvae or loss of blood flow, dying hair cells can be identified
891 several ways: first, by the appearance of karyopyknosis or nuclear condensation, which manifests
892 as a bubble within the cell under DIC optics; second, by cell shrinkage and the presence of rapidly
893 moving particles within the cytoplasm; and third, when kinocilia tips splay out in different
894 directions[35]. When hair bundles are disrupted, the splayed kinocilia do not move cohesively
895 together during stimulation.
896
897 This preparation has several minor limitations, one being that the preparation only remains
898 robust for 1-3 hours after it is established. Modifications such as using smaller pins or a brain-
899 slice harp to immobilize larvae and adding a perfusion system may extend the lifetime of this *in*
900 *vivo* preparation. Another limitation is that photobleaching and phototoxicity can occur after
901 repeated imaging trials. One exciting way to overcome this challenge is to adapt this protocol for
902 light-sheet microscopy. Light-sheet microscopy is a powerful way to reduce out of focus light,
903 leading to less photobleaching and phototoxicity[36]. Together, gentler immobilization and less
904 photo-exposure may help prolong each imaging session. Longer imaging sessions can be used to
905 examine the full duration of functional changes accompanying development and the processes
906 underlying hair-cell clearance and regeneration after injury. It is important to point out that, in
907 addition to light-sheet microscopy, this protocol can be adapted to other types confocal systems
908 (point-scanning, 2-photon, and spinning disk) as well as relatively simple widefield systems[28,34].
909 Overall, its versatility makes this protocol a valuable tool that can be adapted and used with
910 multiple imaging systems.
911
912 While this protocol can be adapted and used with many imaging systems, parts of this protocol
913 can also be adapted and used (1) with other indicators besides GCaMP6s and (2) to image activity
914 in other sensory cells and neurons within larval zebrafish. For example, in a previous study, we
915 used this protocol to image activity using multiple genetically encoded indicators within lateral-
916 line hair cells to detect cytosolic calcium (RGECO1), vesicle fusion (SypHy), membrane voltage
917 (Bongwoori), and membrane calcium (jRCaMP1a-caax and GCaMP6s-caax), and within lateral-
918 line afferent processes to detect membrane calcium (GCaMP6s-caax)[5]. Based on our experience
919 using these indicators, the transgenic line Tg(myo6b:GCaMP6s-caax) described in this protocol
920 offers an excellent start for imaging activity in lateral-line neuromasts. Of all the indicators listed

above, we have found that GCaMP6s is the most sensitive and photostable. In addition to these features, we highlight the Tg(myo6b:GCaMP6s-caax) transgenic line because it can be used to make two distinct measurements: hair-cell mechanosensation and presynaptic calcium within a single transgenic line.

The technique outlined in this article demonstrates how calcium imaging in the zebrafish lateral line can be a powerful method to study how hair cells function in their native environment. This approach is complementary to studies of mammals in which hair-cell function is currently being studied in *ex vivo* explants. In addition, the zebrafish model can continue to be used as a platform to test the efficacy of genetically encoded indicators that can then be applied to examine activity in mammalian hair cells.

DISCLOSURES:
The authors have nothing to disclose.

REFERENCES
1. Russell, J. T. Imaging calcium signals *in vivo*: a powerful tool in physiology and pharmacology. *British Journal of Pharmacology*. **163** (8), 1605–1625, doi: 10.1111/j.1476-5381.2010.00988.x (2011).
2. Pérez Koldenkova, V., Nagai, T. Genetically encoded Ca2+ indicators: Properties and evaluation. *Biochimica et Biophysica Acta (BBA) - Molecular Cell Research*. **1833** (7), 1787–1797, doi: 10.1016/j.bbamcr.2013.01.011 (2013).
3. Lin, M. Z., Schnitzer, M. J. Genetically encoded indicators of neuronal activity. *Nature Neuroscience*. **19** (9), 1142–1153, doi: 10.1038/nn.4359 (2016).
4. Tian, L., Hires, S. A., Looger, L. L. Imaging Neuronal Activity with Genetically Encoded Calcium Indicators. *Cold Spring Harbor Protocols*. **2012** (6), doi: 10.1101/pdb.top069609 (2012).
5. Zhang, Q., *et al.*. Synaptically silent sensory hair cells in zebrafish are recruited after damage. *Nature Communications*. **9** (1), 1388, doi: 10.1038/s41467-018-03806-8 (2018).
6. Harris, G. G., Frishkopf, L. S., Flock, A. Receptor potentials from hair cells of the lateral line. *Science (New York, N.Y.)*. **167** (3914), 76–79 (1970).
7. Eatock, R. A. Vertebrate Hair Cells: Modern and Historic Perspectives. *Vertebrate Hair Cells*. 1–19, doi: 10.1007/0-387-31706-6_1 (2006).
8. World Health Organization Deafness and Hearing Loss, Key Facts. <http://www.who.int/en/news-room/fact-sheets/detail/deafness-and-hearing-loss> (2018).
9. Tang, L. S., Montemayor, C., Pereira, F. A. Sensorineural hearing loss: potential therapies and gene targets for drug development. *IUBMB Life*. **58** (9), 525–530, doi: 10.1080/15216540600913258 (2006).
10. Assad, J. A., Shepherd, G. M. G., Corey, D. P. Tip-link integrity and mechanical transduction in vertebrate hair cells. *Neuron*. **7** (6), 985–994, doi: 10.1016/0896-6273(91)90343-X (1991).

965 11. Lumpkin, E. A., Hudspeth, A. J. Detection of Ca2+ entry through mechanosensitive channels
966 localizes the site of mechanoelectrical transduction in hair cells. *Proceedings of the National*
967 *Academy of Sciences*. **92** (22), 10297–10301, doi: 10.1073/pnas.92.22.10297 (1995).
968 12. Ricci, A. J., Wu, Y. -C., Fettiplace, R. The Endogenous Calcium Buffer and the Time Course of
969 Transducer Adaptation in Auditory Hair Cells. *Journal of Neuroscience*. **18** (20), 8261–8277, doi:
970 10.1523/JNEUROSCI.18-20-08261.1998 (1998).
971 13. Moser, T., Beutner, D. Kinetics of exocytosis and endocytosis at the cochlear inner hair cell
972 afferent synapse of the mouse. *Proceedings of the National Academy of Sciences of the United*
973 *States of America*. **97** (2), 883–888 (2000).
974 14. Brandt, A., Khimich, D., Moser, T. Few CaV1.3 channels regulate the exocytosis of a synaptic
975 vesicle at the hair cell ribbon synapse. *The Journal of Neuroscience: The Official Journal of the*
976 *Society for Neuroscience*. **25** (50), 11577–11585, doi: 10.1523/JNEUROSCI.3411-05.2005 (2005).
977 15. Olt, J., Allen, C. E., Marcotti, W. In vivo physiological recording from the lateral line of juvenile
978 zebrafish. *The Journal of Physiology*. **594** (19), 5427–5438, doi: 10.1113/JP271794 (2016).
979 16. Olt, J., Johnson, S. L., Marcotti, W. In vivo and *in vitro* biophysical properties of hair cells from
980 the lateral line and inner ear of developing and adult zebrafish. *The Journal of Physiology*. **592**
981 (10), 2041–2058, doi: 10.1113/jphysiol.2013.265108 (2014).
982 17. Griguer, C., Fuchs, P. A. Voltage-dependent potassium currents in cochlear hair cells of the
983 embryonic chick. *Journal of Neurophysiology*. **75** (1), 508–513, doi: 10.1152/jn.1996.75.1.508
984 (1996).
985 18. Art, J. J., Fettiplace, R. Variation of membrane properties in hair cells isolated from the turtle
986 cochlea. *The Journal of Physiology*. **385**, 207–242 (1987).
987 19. Goutman, J. D., Pyott, S. J. Whole-Cell Patch-Clamp Recording of Mouse and Rat Inner Hair
988 Cells in the Intact Organ of Corti. *Methods in Molecular Biology (Clifton, N.J.)*. **1427**, 471–485, doi:
989 10.1007/978-1-4939-3615-1_26 (2016).
990 20. Einarsson, R., *et al.* Patch Clamp Recordings in Inner Ear Hair Cells Isolated from Zebrafish.
991 *Journal of Visualized Experiments*. (68), doi: 10.3791/4281 (2012).
992 21. Fuchs, P. A. Time and intensity coding at the hair cell's ribbon synapse. *The Journal of*
993 *Physiology*. **566** (Pt 1), 7–12, doi: 10.1113/jphysiol.2004.082214 (2005).
994 22. Moser, T., Brandt, A., Lysakowski, A. Hair cell ribbon synapses. *Cell and Tissue Research*. **326**
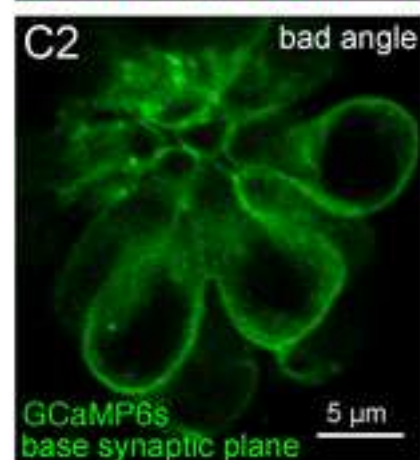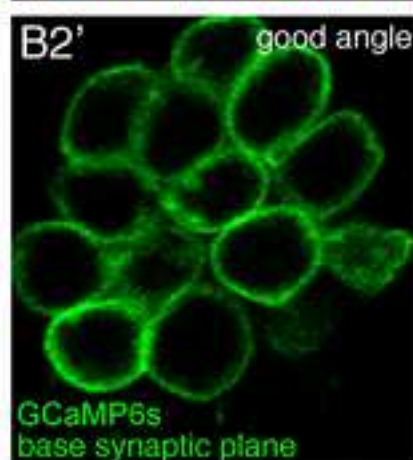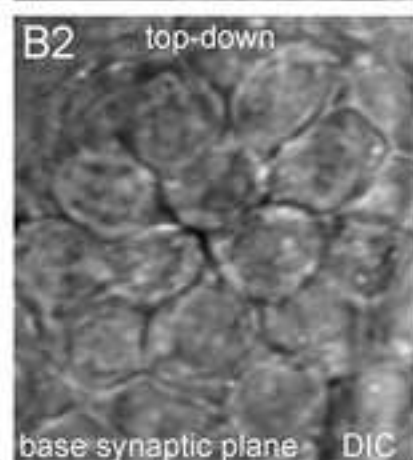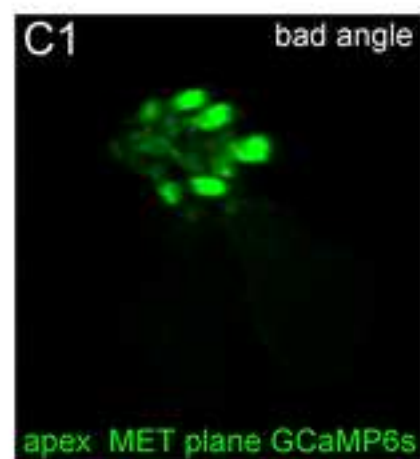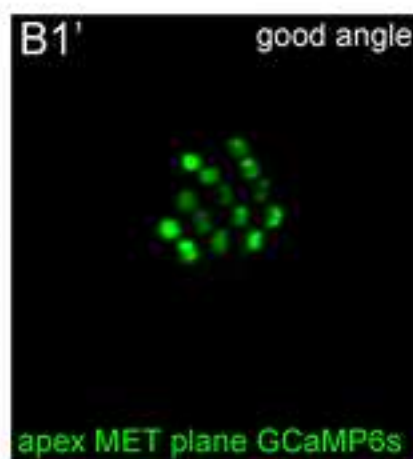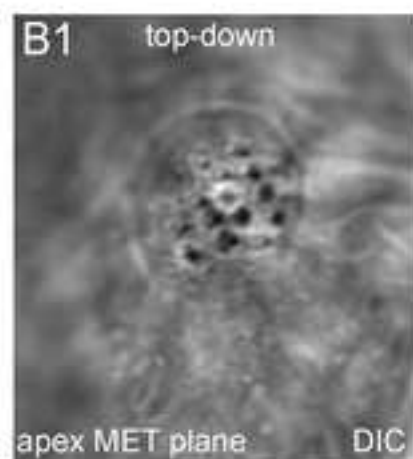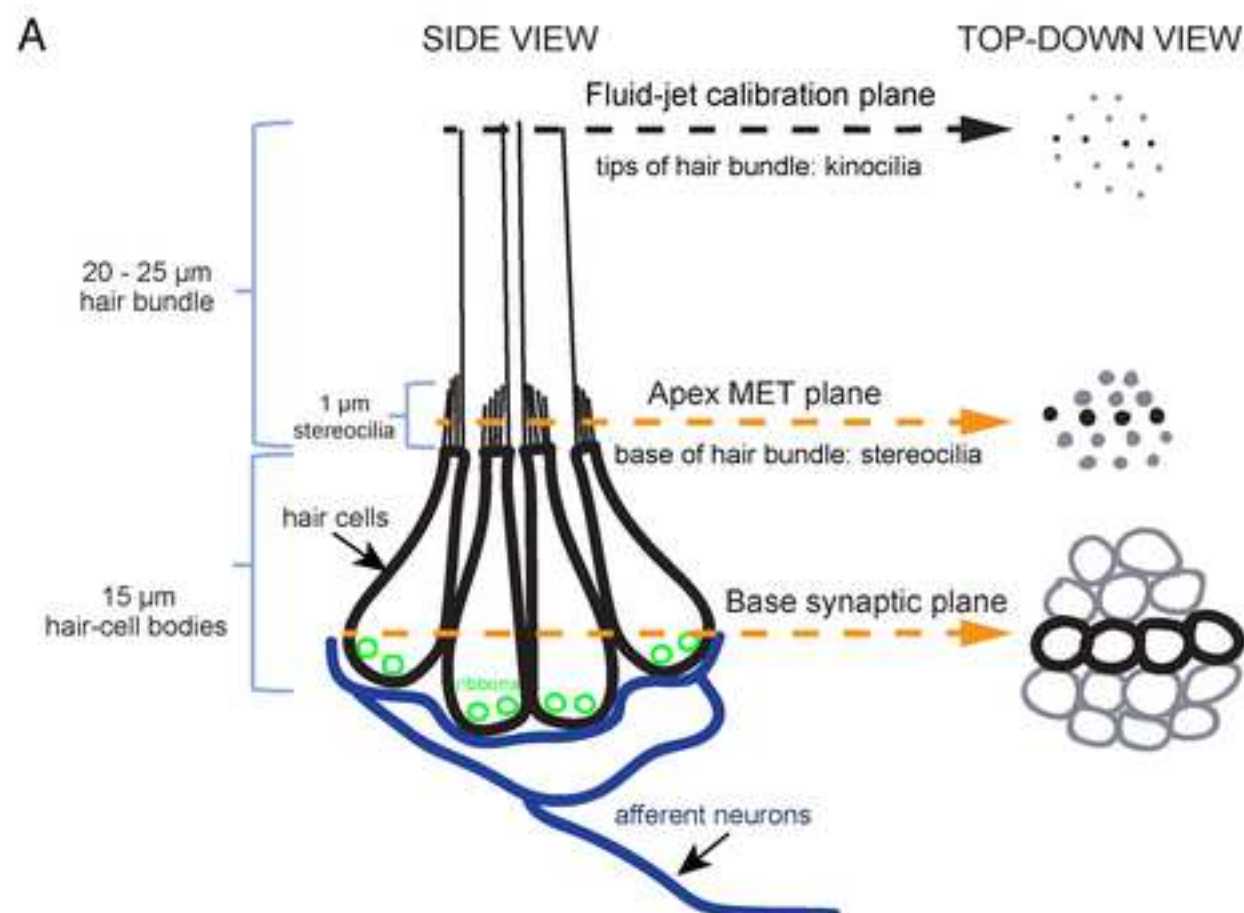995 (2), 347–359, doi: 10.1007/s00441-006-0276-3 (2006).
996 23. Trapani, J. G., Nicolson, T. Chapter 8 - Physiological Recordings from Zebrafish Lateral-Line
997 Hair Cells and Afferent Neurons. *Methods in Cell Biology*. **100**, 219–231, doi: 10.1016/B978-0-12-
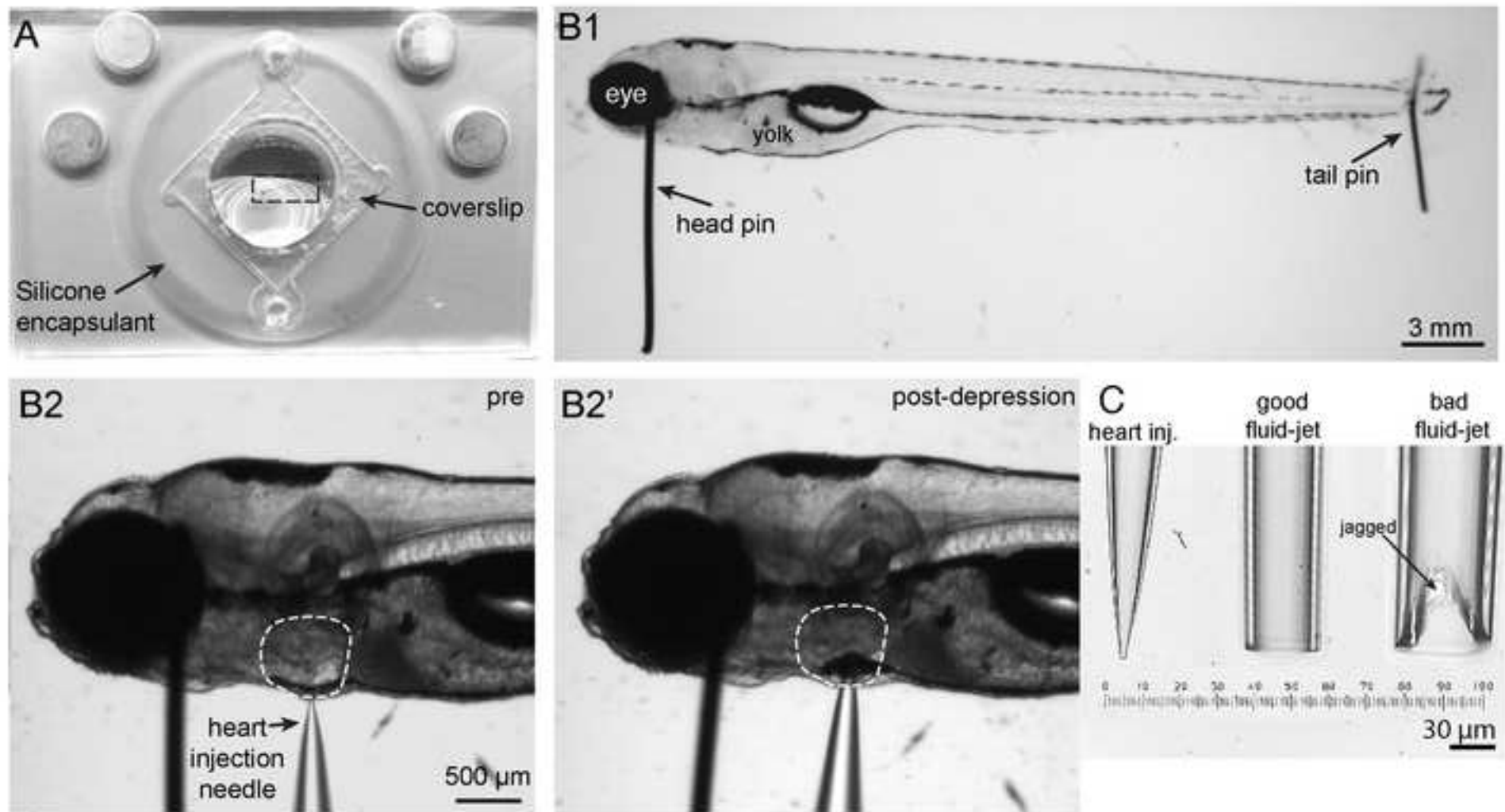998 384892-5.00008-6 (2010).
999 24. Olt, J., Ordoobadi, A. J., Marcotti, W., Trapani, J. G. Physiological recordings from the
1000 zebrafish lateral line. *Methods in Cell Biology*. **133**, 253–279, doi: 10.1016/bs.mcb.2016.02.004
1001 (2016).
1002 25. Stawicki, T. M., Esterberg, R., Hailey, D. W., Raible, D. W., Rubel, E. W. Using the zebrafish
1003 lateral line to uncover novel mechanisms of action and prevention in drug-induced hair cell
1004 death. *Frontiers in Cellular Neuroscience*. **9**, doi: 10.3389/fncel.2015.00046 (2015).
1005 26. Spinelli, K. J., Gillespie, P. G. Monitoring Intracellular Calcium Ion Dynamics in Hair Cell
1006 Populations with Fluo-4 AM. *PLOS ONE*. **7** (12), e51874, doi: 10.1371/journal.pone.0051874
1007 (2012).

1008   27. Kwan, K.M., *et al.* The Tol2kit: a multisite gateway-based construction kit for Tol2 transposon
1009   transgenesis constructs. *Developmental Dynamics: An Official Publication of the American*
1010   *Association of Anatomists*. **236** (11), 3088–3099, doi: 10.1002/dvdy.21343 (2007).

1011   28. Zhang, Q. X., He, X. J., Wong, H. C., Kindt, K. S. Chapter 10 - Functional calcium imaging in
1012   zebrafish lateral-line hair cells. *Methods in Cell Biology*. **133**, 229–252, doi:
1013   10.1016/bs.mcb.2015.12.002 (2016).

1014   29. Sheets, L., *et al.* Enlargement of Ribbons in Zebrafish Hair Cells Increases Calcium Currents
1015   But Disrupts Afferent Spontaneous Activity and Timing of Stimulus Onset. *The Journal of*
1016   *Neuroscience: The Official Journal of the Society for Neuroscience*. **37** (26), 6299–6313, doi:
1017   10.1523/JNEUROSCI.2878-16.2017 (2017).

1018   30. Zhang, Q. X., He, X. J., Wong, H. C., Kindt, K. S. Functional calcium imaging in zebrafish lateral-
1019   line hair cells. <http://www.sciencedirect.com/science/article/pii/S0091679X15002332>.

1020   31. Chou, S. -W., *et al.* A molecular basis for water motion detection by the mechanosensory
1021   lateral line of zebrafish. *Nature Communications*. **8** (1), 2234, doi: 10.1038/s41467-017-01604-2
1022   (2017).

1023   32. Thevenaz, P., Ruttimann, U. E., Unser, M. A pyramid approach to subpixel registration based
1024   on intensity. *IEEE Transactions on Image Processing*. **7** (1), 27–41, doi: 10.1109/83.650848 (1998).

1025   33. Fiji is just ImageJ. at <https://fiji.sc/>.

1026   34. Esterberg, R., Hailey, D. W., Coffin, A. B., Raible, D. W., Rubel, E. W. Disruption of intracellular
1027   calcium regulation is integral to aminoglycoside-induced hair cell death. *The Journal of*
1028   *Neuroscience: The Official Journal of the Society for Neuroscience*. **33** (17), 7513–7525, doi:
1029   10.1523/JNEUROSCI.4559-12.2013 (2013).

1030   35. Stengel, D., Zindler, F., Braunbeck, T. An optimized method to assess ototoxic effects in the
1031   lateral line of zebrafish (Danio rerio) embryos. *Comparative Biochemistry and Physiology Part C:*
1032   *Toxicology & Pharmacology*. **193**, 18–29, doi: 10.1016/j.cbpc.2016.11.001 (2017).

1033   36. Fadero, T.C., *et al.* LITE microscopy: Tilted light-sheet excitation of model organisms offers
1034   high resolution and low photobleaching. *Journal of Cell Biology*. jcb.201710087, doi:
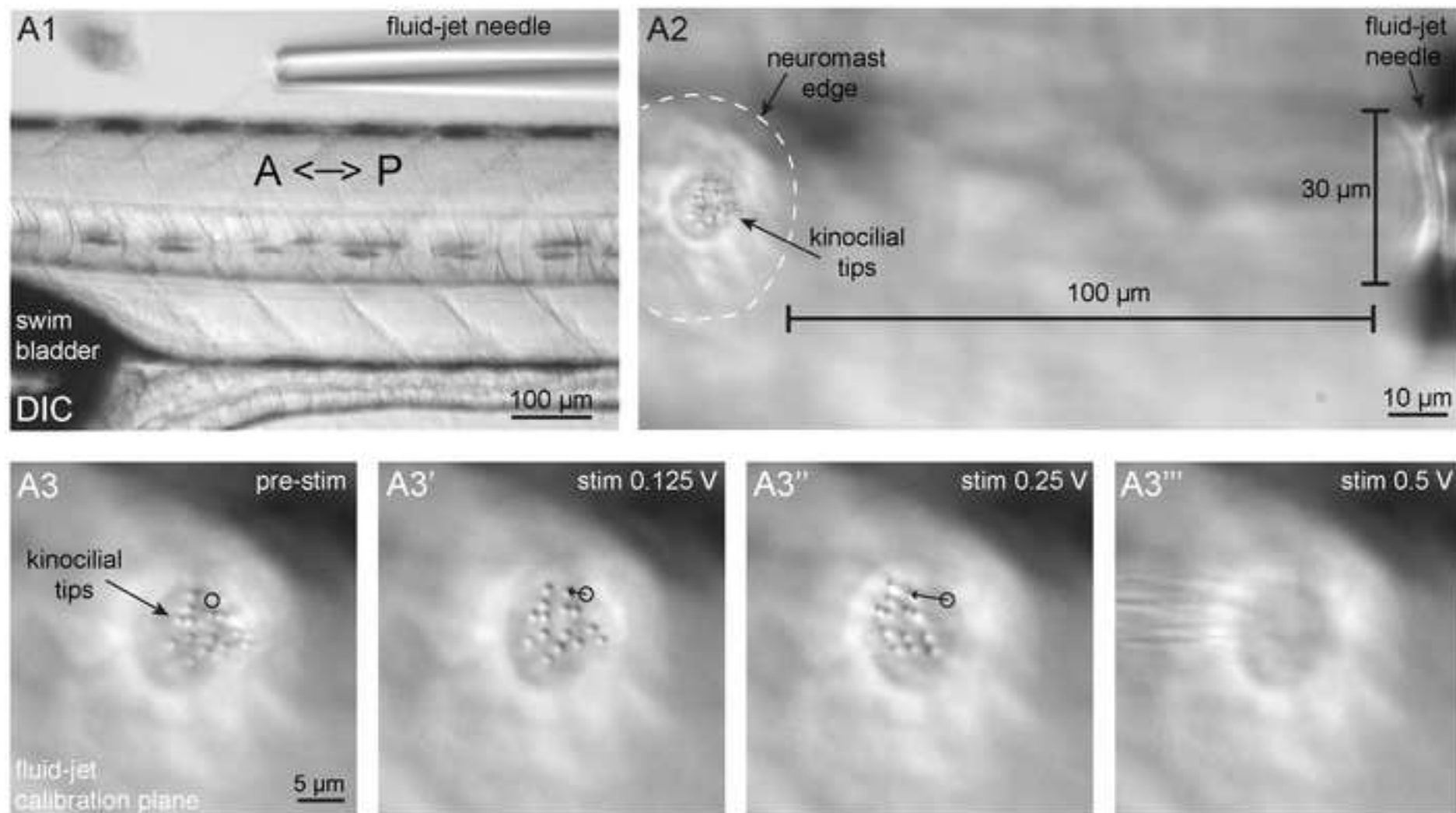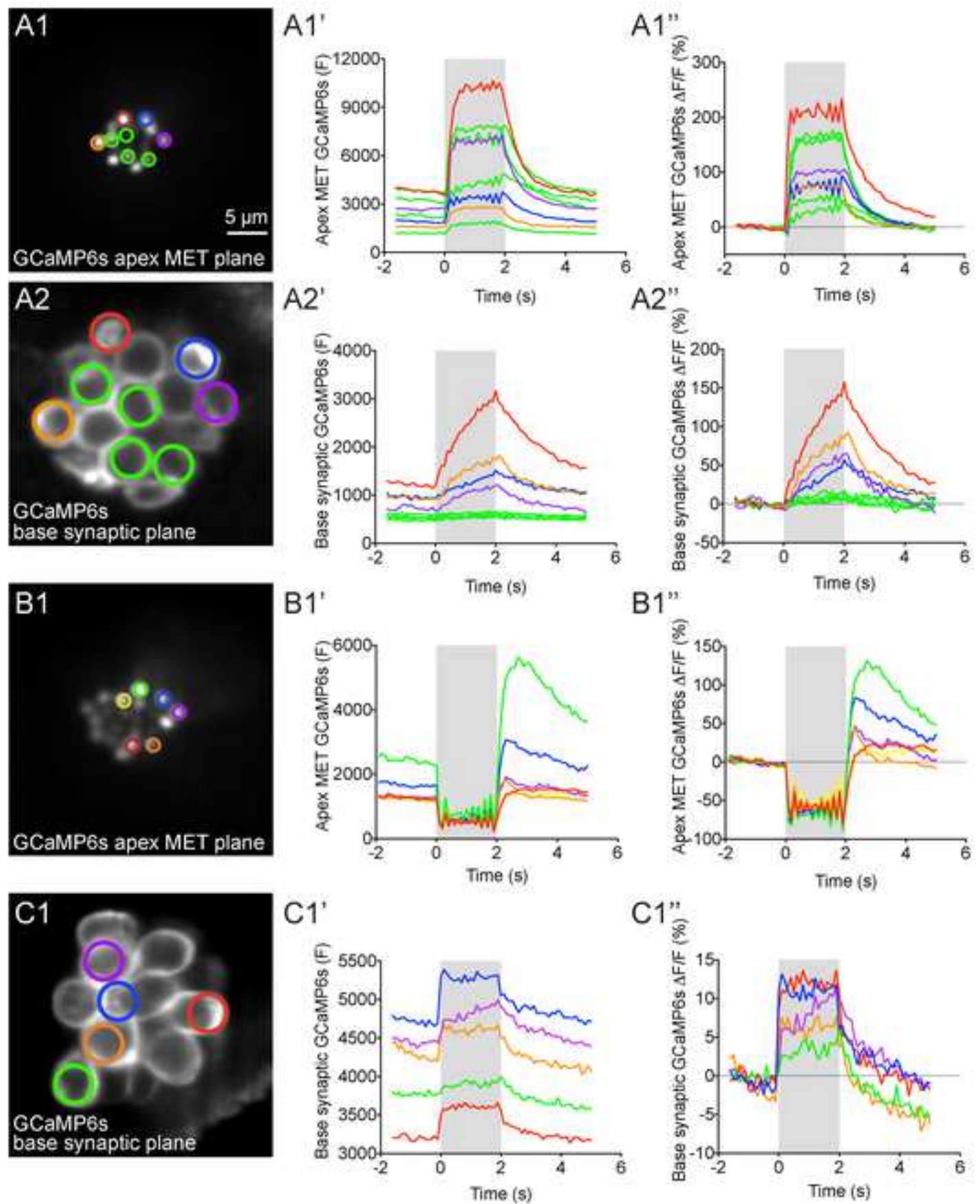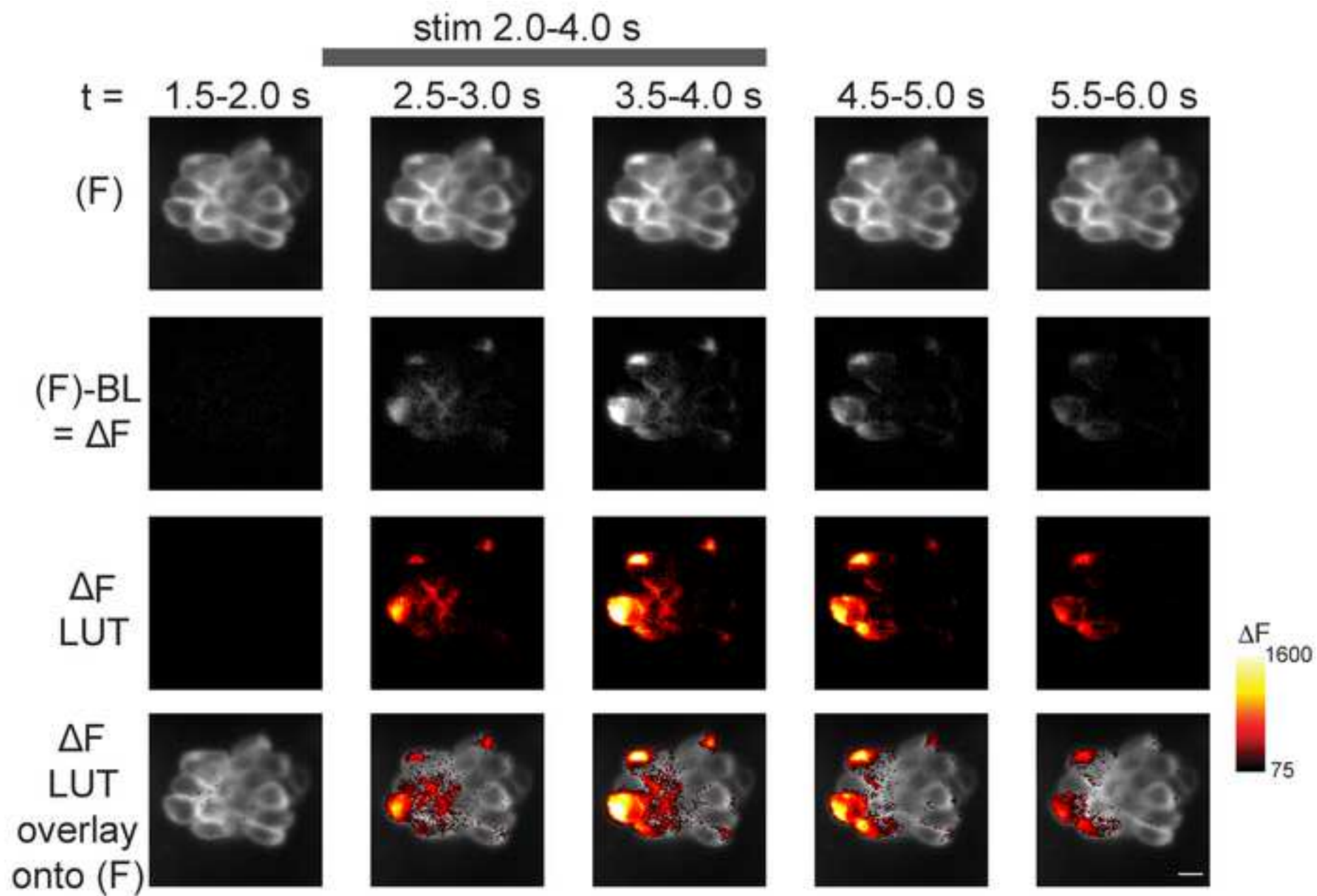1035   10.1083/jcb.201710087 (2018).

Figure 1

A — SIDE VIEW / TOP-DOWN VIEW

Fluid-jet calibration plane
tips of hair bundle: kinocilia
20 - 25 µm hair bundle
1 µm stereocilia
Apex MET plane
base of hair bundle: stereocilia
hair cells
15 µm hair-cell bodies
Base synaptic plane
ribbons
afferent neurons

B1 top-down — apex MET plane DIC
B1' good angle — apex MET plane GCaMP6s
C1 bad angle — apex MET plane GCaMP6s
B2 top-down — base synaptic plane DIC
B2' good angle — GCaMP6s base synaptic plane
C2 bad angle — GCaMP6s base synaptic plane
5 µm

A. Silicone encapsulant, coverslip

B1. eye, yolk, head pin, tail pin, 3 mm

B2. pre, heart injection needle, 500 μm

B2'. post-depression

C. heart inj., good fluid-jet, bad fluid-jet, jagged, 30 μm

Figure 3

stim 2.0-4.0 s

t = 1.5-2.0 s | 2.5-3.0 s | 3.5-4.0 s | 4.5-5.0 s | 5.5-6.0 s

(F)

(F)-BL = ΔF

ΔF LUT

ΔF LUT overlay onto (F)

ΔF 1600

75

Table of Materials

Click here to access/download;Table of Materials;Table of Materials_180823.xls ⬇

Name	Company	Catalog Number	Comments
Section 1			
α-Bungarotoxin	R&D Systems	2133	For paralyzing larvae prior to imaging
Phenol red Solution 0.5%	Sigma-Aldrich	P0290	For visualization of α-bungarotoxin solution during heart injection
Ethyl 3-aminobenzoate methanesulfonate (MESAB, MS-222, tricaine)	Sigma-Aldrich	A5040	For anesthetizing larvae
Section 2			
Imaging chamber	Siskiyou	PC-R	Platform to mount larvae for imaging
No. 1.5 Coverslips square, 22*22 mm	VWR	48366-227	To seal imaging chamber
High vacuum silicone grease	Fischer Scientific	14-635-5D	For affixing of coverslip to imaging chamber
Silicone encapsulant clear 0.5 g kit	Ellsworth Adhesives	Dow Corning Sylgard, 184 SIL ELAST KIT 0.5KG	To fill imaging chamber to create a surface to pin fish
Oven	Techne	HB-1D	For drying silicone encapsulant
Stereomicroscope	Carl Zeiss Microscopy	Stemi 2000 with transmitted light illumination	For illuminating wire, forceps and scissors to make pins
Fine forceps	Fine Science Tools	Dumont #5 (0.05 x 0.02 mm) Item No. 11295-10	For making pins
Fine scissors	Cole-Palmer	5.5", EW-10818-00	For cutting tunsgten wire to make pins
Tungsten wire, 0.035 mm	Goodfellow	W005131	For head pins to immobilize larvae
Tungsten wire, 0.025 mm	ThermoFischer Scientific	AA10405-H4	For tail pins to immobilize larvae
Section 3			
Micropipette guller	Sutter Instrument Company	P-97	For pulling capillary glass for fluid-jet and heart injection needles
Borosilicate glass capillaries w/ filament	Sutter Instrument Company	BF 150-86-10	Glass to be pulled into α-bungarotoxin injection needles for heart injection
Borosilicate glass capillaries w/o filament	Sutter Instrument Company	B 150-86-10	Glass to be pulled into fluid-jet needles to stimulate hair cells
Pipette polisher	Narishige	MF-830 microforge	To polish fluid-jet pipette tips to smooth jagged breaks
Ceramic tile	Sutter Instrument Company	NC9569052	For scoring and evening breaking fluid-jet needles
Sections 4 & 5			
Fine forceps	Fine Science Tools	Dumont #5 (0.05 x 0.02 mm) Item No. 11295-10	For pinning larvae
Gel loading tips	Eppendorf	5242956003	For backfilling heart injection needles
Stereomicroscope	Carl Zeiss Microscopy	Stemi 2000 with transmitted light illumination	For illuminating larvae during pinning and heart injection
Glass capillary/needle holder	WPI	MPH315	To hold fluid-jet needles
Manual micromanipulator	Narishige	M-152	For holding and positioning of needle holder to inject α-bungarotoxin
Magnetic stand	Narishige	GJ-1	For holding manual micromanipulator for α-bungarotoxin injection
Pressure injector	Eppendorf	Femtojet 4x	To deliver α-bungarotoxin
Sections 6, 7 & 8			
Confocal microscope	Bruker	Swept field/Opterra confocal microscope	Fixed, upright microscope with DIC optics and 488nm laser with appropriate filters
Microscope software	Bruker	Prairieview 5.3	To coordinate and control the microscope, lasers, stage, piezo-z, cameras and fluid jet
10X air objective	Nikon	MRH00101	Low magnification for positioning of larvae and fluid jet
60X water objective	Nikon	MRF07620	Water immerison objective with high NA (1.0) and adequate working distance (2.0 mm)
Piezo-Z objective scanner with controller/driver	Physik Intruments instruments/Bruker	01144210/UM-Z-PZ	High-speed z-stack acquisition with 0.025um accuracy
EMCCD camera	QImaging	Rolera EM-C2 EMCCD camera	Camera with small pixel size that can acquire up to 100 frames per s
Circular chamber adapter	Siskiyou	PC-A	For holding and rotating imaging chamber on microscope stage
Motorized Z-deck stage	Prior Scientific	ZDN12MP	Microscope stage that can hold and move sample and micromanipulator with fluid-jet needle together
Z-deck stage insert adaptor	NIH Machine shop	custom	To fit the circular chamber adaptor onto the z-deck stage
Fluid-jet apparatus	ALA scientific instruments	HSPC-1 High-speed pressure Clamp with PV-PUMP	For controlling and delivering the fluid-jet stimulus
Masterflex Peroxide-cured silicone tubing (1 ft)	Cole-Palmer	Masterflex L/S 13, 96400-13	For connecting the fluid-jet needle holder to pressure pump
Motorized micromanipulator	Sutter Instrument Company	MP-225	For holding and positioning of needle holder for fluid jet
Micromanipulator controller	Sutter Instrument Company	MPC-200	For controlling fluid-jet needle manipulator
Gel loading tips	Eppendorf	5242956003	For backfilling fluid-jet needles
Glass capillary/needle holder	WPI	MPH315	To hold fluid-jet needles
PSI manometer	Sper Scientific	840081	For measuring pressure clamp output
Section 9			
BAPTA, Tetrapotassium Salt, cell impermeant	ThermoFischer Scientific	B1204	To cleave tips links, uncouple MET channels and block all evoked GCaMP6s signals
Isradipine	Sigma-Aldrich	I6658	To block signals dependent on the L-type calcium channels (CaV1.3) at the presynapse
DMSO	Sigma-Aldrich	D8418	Solvent for pharmacological compounds
Section 10			
Prism7	Graphpad	Prism7	Software to plot GCaMP6 intensity changes
FIJI	Schindelin, et., al.[34]	https://fiji.sc/	Software to process images and create spatio-temporal signal maps
Turboreg Plugin	Thévenaz et., al.[29]	http://bigwww.epfl.ch/thevenaz/turboreg/	Plugin to register GCaMP6 image sequences in FIJI
StackReg Plugin	Thévenaz et., al.[29]	http://bigwww.epfl.ch/thevenaz/stackreg/	Plugin to register GCaMP6 image sequences in FIJI
Times Series Analyzer V3 Plugin	Balaji J 2007, Dept. of Neurobiology, UCLA	https://imagej.nih.gov/ij/plugins/time-series.html	Plugin to create multiple ROIs to measure GCaMP6 intensity changes

NIH Publishing Agreement & Manuscript *Cover Sheet*

By signing this Cover Sheet, the Author, on behalf of NIH, agrees to the provisions set out below, which **modify and supersede,** solely with respect to NIH, any conflicting provisions that are in the Publisher's standard copyright agreement (the "Publisher's Agreement"). If a Publisher's Agreement is attached, execution of this Cover Sheet constitutes an execution of the Publisher's Agreement, subject to the provisions and conditions of this Cover Sheet.

1. **Indemnification.** No Indemnification or "hold harmless" obligation is provided by either party.

2. **Governing Law.** This agreement will be governed by the law of the court in which a claim is brought.

3. **Copyright.** Author's contribution to the Work was done as part of the Author's official duties as a NIH employee and is a Work of the United States Government. Therefore, copyright may not be established in the United States. 17 U.S.C. § 105. If Publisher intends to disseminate the Work outside of the U.S., Publisher may secure copyright to the extent authorized under the domestic laws of the relevant country, subject to a paid-up, nonexclusive, irrevocable worldwide license to the United States in such copyrighted work to reproduce, prepare derivative works, distribute copies to the public and perform publicly and display publicly the work, and to permit others to do so.

4. **No Compensation.** No royalty income or other compensation may be accepted for work done as part of official duties. The author may accept for the agency a limited number of reprints or copies of the publication.

5. **NIH Representations.** NIH represents to the Publisher that the Author is the sole author of the Author's contribution to the Work and that NIH is the owner of the rights that are the subject of this agreement; that the Work is an original work and has not previously been published in any form anywhere in the world; that to the best of NIH's knowledge the Work is not a violation of any existing copyright, moral right, database right, or of any right of privacy or other intellectual property, personal, proprietary or statutory right; that where the Author is responsible for obtaining permissions or assisting the Publishers in obtaining permissions for the use of third party material, all relevant permissions and information have been secured; and that the Work contains nothing misleading, obscene, libelous or defamatory or otherwise unlawful. NIH agrees to reasonable instructions or requirements regarding submission procedures or author communications, and reasonable ethics or conflict of interest disclosure requirements unless they conflict with the provisions of this Cover Sheet.

6. **Disclaimer.** NIH and the Author expressly disclaim any obligation in Publisher's Agreement that is not consistent with the Author's official duties or the NIH mission, described at http://www.nih.gov/about/. NIH and the Author do not disclaim obligations to comply with a Publisher's conflict of interest policy so long as, and to the extent that, such policy is consistent with NIH's own conflict of interest policies.

7. **For Peer-Reviewed Papers to be Submitted to PubMed Central.** The Author is a US government employee who must comply with the NIH Public Access Policy, and the Author or NIH will deposit, or have deposited, in NIH's PubMed Central archive, an electronic version of the final, peer-reviewed manuscript upon acceptance for publication, to be made publicly available no later than 12 months after the official date of publication. The Author and NIH agree (notwithstanding Paragraph 3 above) to follow the manuscript deposition procedures (including the relevant embargo period, if any) of the publisher so long as they are consistent with the NIH Public Access Policy.

8. **Modifications.** PubMed Central may tag or modify the work consistent with its customary practices and with the meaning and integrity of the underlying work.

The NIH Deputy Director for Intramural Research, Michael Gottesman, M.D., approves this publishing agreement and maintains a single, signed copy of this text for all works published by NIH employees, and contractors and trainees who are working at the NIH. No additional signature from Dr. Gottesman is needed.

Author's name: **Katie Kindt**

Author's Institute or Center: **National Institutes of Health**   Check if Publisher' Agreement is attached ☐

Name of manuscript/work: **Protocol for live imaging of mechanosensation- and presynapse-dependent calciu**

Name of publication: **JoVE**

_____
Author's signature

7-16-18
_____
Date

jove
JOURNAL OF
VISUALIZED EXPERIMENTS

1 Alewife Center #200
Cambridge, MA 02140
tel. 617.945.9051
www.jove.com

ARTICLE AND VIDEO LICENSE AGREEMENT

Title of Article:

Protocol for live imaging of mechanosensation- and presynapse-dependent calcium responses in lateral-line hair cells of larval zebrafish (Danio rerio).

Author(s):

Daria Lukasz and Katie S. Kindt

Item 1: The Author elects to have the Materials be made available (as described at http://www.jove.com/publish) via:

☐ Standard Access   ☒ Open Access

Item 2: Please select one of the following items:

☐ The Author is **NOT** a United States government employee.

☒ The Author is a United States government employee and the Materials were prepared in the course of his or her duties as a United States government employee.

☐ The Author is a United States government employee but the Materials were NOT prepared in the course of his or her duties as a United States government employee.

ARTICLE AND VIDEO LICENSE AGREEMENT

1.   **Defined Terms.** As used in this Article and Video License Agreement, the following terms shall have the following meanings: "**Agreement**" means this Article and Video License Agreement; "**Article**" means the article specified on the last page of this Agreement, including any associated materials such as texts, figures, tables, artwork, abstracts, or summaries contained therein; "**Author**" means the author who is a signatory to this Agreement; "**Collective Work**" means a work, such as a periodical issue, anthology or encyclopedia, in which the Materials in their entirety in unmodified form, along with a number of other contributions, constituting separate and independent works in themselves, are assembled into a collective whole; "**CRC License**" means the Creative Commons Attribution-Non Commercial-No Derivs 3.0 Unported Agreement, the terms and conditions of which can be found at: http://creativecommons.org/licenses/by-nc-nd/3.0/legalcode; "**Derivative Work**" means a work based upon the Materials or upon the Materials and other pre-existing works, such as a translation, musical arrangement, dramatization, fictionalization, motion picture version, sound recording, art reproduction, abridgment, condensation, or any other form in which the Materials may be recast, transformed, or adapted; "**Institution**" means the institution, listed on the last page of this Agreement, by which the Author was employed at the time of the creation of the Materials; "**JoVE**" means MyJove Corporation, a Massachusetts corporation and the publisher of The Journal of Visualized Experiments; "**Materials**" means the Article and / or the Video; "**Parties**" means the Author and JoVE; "**Video**" means any video(s) made by the Author, alone or in conjunction with any other parties, or by JoVE or its affiliates or agents, individually or in collaboration with the Author or any other parties, incorporating all or any portion

of the Article, and in which the Author may or may not appear.

2.   **Background.** The Author, who is the author of the Article, in order to ensure the dissemination and protection of the Article, desires to have the JoVE publish the Article and create and transmit videos based on the Article. In furtherance of such goals, the Parties desire to memorialize in this Agreement the respective rights of each Party in and to the Article and the Video.

3.   **Grant of Rights in Article.** In consideration of JoVE agreeing to publish the Article, the Author hereby grants to JoVE, subject to **Sections 4** and **7** below, the exclusive, royalty-free, perpetual (for the full term of copyright in the Article, including any extensions thereto) license (a) to publish, reproduce, distribute, display and store the Article in all forms, formats and media whether now known or hereafter developed (including without limitation in print, digital and electronic form) throughout the world, (b) to translate the Article into other languages, create adaptations, summaries or extracts of the Article or other Derivative Works (including, without limitation, the Video) or Collective Works based on all or any portion of the Article and exercise all of the rights set forth in (a) above in such translations, adaptations, summaries, extracts, Derivative Works or Collective Works and (c) to license others to do any or all of the above. The foregoing rights may be exercised in all media and formats, whether now known or hereafter devised, and include the right to make such modifications as are technically necessary to exercise the rights in other media and formats. If the "Open Access" box has been checked in **Item 1** above, JoVE and the Author hereby grant to the public all such rights in the Article as provided in, but subject to all limitations and requirements set forth in, the CRC License.

4. **Retention of Rights in Article.** Notwithstanding the exclusive license granted to JoVE in **Section 3** above, the Author shall, with respect to the Article, retain the non-exclusive right to use all or part of the Article for the non-commercial purpose of giving lectures, presentations or teaching classes, and to post a copy of the Article on the Institution's website or the Author's personal website, in each case provided that a link to the Article on the JoVE website is provided and notice of JoVE's copyright in the Article is included. All non-copyright intellectual property rights in and to the Article, such as patent rights, shall remain with the Author.

5. **Grant of Rights in Video – Standard Access.** This **Section 5** applies if the "Standard Access" box has been checked in **Item 1** above or if no box has been checked in **Item 1** above. In consideration of JoVE agreeing to produce, display or otherwise assist with the Video, the Author hereby acknowledges and agrees that, Subject to **Section 7** below, JoVE is and shall be the sole and exclusive owner of all rights of any nature, including, without limitation, all copyrights, in and to the Video. To the extent that, by law, the Author is deemed, now or at any time in the future, to have any rights of any nature in or to the Video, the Author hereby disclaims all such rights and transfers all such rights to JoVE.

6. **Grant of Rights in Video – Open Access.** This **Section 6** applies only if the "Open Access" box has been checked in **Item 1** above. In consideration of JoVE agreeing to produce, display or otherwise assist with the Video, the Author hereby grants to JoVE, subject to **Section 7** below, the exclusive, royalty-free, perpetual (for the full term of copyright in the Article, including any extensions thereto) license (a) to publish, reproduce, distribute, display and store the Video in all forms, formats and media whether now known or hereafter developed (including without limitation in print, digital and electronic form) throughout the world, (b) to translate the Video into other languages, create adaptations, summaries or extracts of the Video or other Derivative Works or Collective Works based on all or any portion of the Video and exercise all of the rights set forth in (a) above in such translations, adaptations, summaries, extracts, Derivative Works or Collective Works and (c) to license others to do any or all of the above. The foregoing rights may be exercised in all media and formats, whether now known or hereafter devised, and include the right to make such modifications as are technically necessary to exercise the rights in other media and formats. For any Video to which this **Section 6** is applicable, JoVE and the Author hereby grant to the public all such rights in the Video as provided in, but subject to all limitations and requirements set forth in, the CRC License.

7. **Government Employees.** If the Author is a United States government employee and the Article was prepared in the course of his or her duties as a United States government employee, as indicated in **Item 2** above, and any of the licenses or grants granted by the Author hereunder exceed the scope of the 17 U.S.C. 403, then the rights granted hereunder shall be limited to the maximum rights permitted under such statute. In such case, all provisions contained herein that are not in conflict with such statute shall remain in full force and effect, and all provisions contained herein that do so conflict shall be deemed to be amended so as to provide to JoVE the maximum rights permissible within such statute.

8. **Protection of the Work.** The Author(s) authorize JoVE to take steps in the Author(s) name and on their behalf if JoVE believes some third party could be infringing or might infringe the copyright of either the Author's Article and/or Video.

9. **Likeness, Privacy, Personality.** The Author hereby grants JoVE the right to use the Author's name, voice, likeness, picture, photograph, image, biography and performance in any way, commercial or otherwise, in connection with the Materials and the sale, promotion and distribution thereof. The Author hereby waives any and all rights he or she may have, relating to his or her appearance in the Video or otherwise relating to the Materials, under all applicable privacy, likeness, personality or similar laws.

10. **Author Warranties.** The Author represents and warrants that the Article is original, that it has not been published, that the copyright interest is owned by the Author (or, if more than one author is listed at the beginning of this Agreement, by such authors collectively) and has not been assigned, licensed, or otherwise transferred to any other party. The Author represents and warrants that the author(s) listed at the top of this Agreement are the only authors of the Materials. If more than one author is listed at the top of this Agreement and if any such author has not entered into a separate Article and Video License Agreement with JoVE relating to the Materials, the Author represents and warrants that the Author has been authorized by each of the other such authors to execute this Agreement on his or her behalf and to bind him or her with respect to the terms of this Agreement as if each of them had been a party hereto as an Author. The Author warrants that the use, reproduction, distribution, public or private performance or display, and/or modification of all or any portion of the Materials does not and will not violate, infringe and/or misappropriate the patent, trademark, intellectual property or other rights of any third party. The Author represents and warrants that it has and will continue to comply with all government, institutional and other regulations, including, without limitation all institutional, laboratory, hospital, ethical, human and animal treatment, privacy, and all other rules, regulations, laws, procedures or guidelines, applicable to the Materials, and that all research involving human and animal subjects has been approved by the Author's relevant institutional review board.

11. **JoVE Discretion.** If the Author requests the assistance of JoVE in producing the Video in the Author's facility, the Author shall ensure that the presence of JoVE employees, agents or independent contractors is in accordance with the relevant regulations of the Author's institution. If more than one author is listed at the beginning of this Agreement, JoVE may, in its sole

discretion, elect not take any action with respect to the Article until such time as it has received complete, executed Article and Video License Agreements from each such author. JoVE reserves the right, in its absolute and sole discretion and without giving any reason therefore, to accept or decline any work submitted to JoVE. JoVE and its employees, agents and independent contractors shall have full, unfettered access to the facilities of the Author or of the Author's institution as necessary to make the Video, whether actually published or not. JoVE has sole discretion as to the method of making and publishing the Materials, including, without limitation, to all decisions regarding editing, lighting, filming, timing of publication, if any, length, quality, content and the like.

12. **Indemnification.** The Author agrees to indemnify JoVE and/or its successors and assigns from and against any and all claims, costs, and expenses, including attorney's fees, arising out of any breach of any warranty or other representations contained herein. The Author further agrees to indemnify and hold harmless JoVE from and against any and all claims, costs, and expenses, including attorney's fees, resulting from the breach by the Author of any representation or warranty contained herein or from allegations or instances of violation of intellectual property rights, damage to the Author's or the Author's institution's facilities, fraud, libel, defamation, research, equipment, experiments, property damage, personal injury, violations of institutional, laboratory, hospital, ethical, human and animal treatment, privacy or other rules, regulations, laws, procedures or guidelines, liabilities and other losses or damages related in any way to the submission of work to JoVE, making of videos by JoVE, or publication in JoVE or elsewhere by JoVE. The Author shall be responsible for, and shall hold JoVE harmless from, damages caused by lack of sterilization, lack of cleanliness or by contamination due to
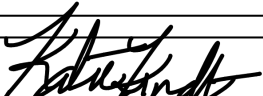
the making of a video by JoVE its employees, agents or independent contractors. All sterilization, cleanliness or decontamination procedures shall be solely the responsibility of the Author and shall be undertaken at the Author's expense. All indemnifications provided herein shall include JoVE's attorney's fees and costs related to said losses or damages. Such indemnification and holding harmless shall include such losses or damages incurred by, or in connection with, acts or omissions of JoVE, its employees, agents or independent contractors.

13. **Fees.** To cover the cost incurred for publication, JoVE must receive payment before production and publication the Materials. Payment is due in 21 days of invoice. Should the Materials not be published due to an editorial or production decision, these funds will be returned to the Author. Withdrawal by the Author of any submitted Materials after final peer review approval will result in a US$1,200 fee to cover pre-production expenses incurred by JoVE. If payment is not received by the completion of filming, production and publication of the Materials will be suspended until payment is received.

14. **Transfer, Governing Law.** This Agreement may be assigned by JoVE and shall inure to the benefits of any of JoVE's successors and assignees. This Agreement shall be governed and construed by the internal laws of the Commonwealth of Massachusetts without giving effect to any conflict of law provision thereunder. This Agreement may be executed in counterparts, each of which shall be deemed an original, but all of which together shall be deemed to me one and the same agreement. A signed copy of this Agreement delivered by facsimile, e-mail or other means of electronic transmission shall be deemed to have the same legal effect as delivery of an original signed copy of this Agreement.

A signed copy of this document must be sent with all new submissions. Only one Agreement is required per submission.

CORRESPONDING AUTHOR

Name: Katie S. Kindt

Department: National Institute on Deafness and other communication disorders

Institution: National Institutes of Health

Title: Investigator

Signature: _[signature]_   Date: 7-17-18

Please submit a **signed** and **dated** copy of this license by one of the following three methods:
1. Upload an electronic version on the JoVE submission site
2. Fax the document to +1.866.381.2236
3. Mail the document to JoVE / Attn: JoVE Editorial / 1 Alewife Center #200 / Cambridge, MA 02140

612542.6   For questions, please contact us at submissions@jove.com or +1.617.945.9051.

We would like to thank the editors and the reviewers for their helpful comments to improve our protocol.
NOTE: We have removed any line numbers that the reviewers themselves referenced in their comments from this document since those numbers refer back to an earlier version. Any line numbers referenced in this document refer to the edited version (not the clean version) of the document that we are resubmitting along with these comments.

Editorial comments:
Changes to be made by the Author(s) regarding the written manuscript:
1. Please take this opportunity to thoroughly proofread the manuscript to ensure that there are no spelling or grammar issues.
We have done our best to proofread the manuscript.
2. Please remove the embedded figure(s) and Table of Materials from the manuscript.
We have removed the embedded figure(s) and Table of Materials from the manuscript.
3. Please upload each Figure individually to your Editorial Manager account as a .png, .tiff, .svg, .eps, .psd, or .ai file.
Done.
4. Figure 1: Please note that Figure 1 embedded in the manuscript (page 17) and Figure 1 uploaded separately (page 30) are not the same. Please upload a final version of Figure 1 that matches the Figure 1 legend and has its scale bar defined in the figure or its figure legend.
We now have just one final Figure 1 image. The scale bar is defined in the figure and legend.
5. Figure 4: Please change the time unit "sec" to "s".
The graphs now use "s".
6. Please shorten the title if possible.
We have shortened the title.
7. Please provide an email address for each author.
We have provided an email address for each author (lines 6-7).
8. Keywords: Please provide at least 6 keywords or phrases.
We have provided keywords (lines 17-18).
9. Please revise the protocol to contain only action items that direct the reader to do something (e.g., "Do this," "Ensure that," etc.). The actions should be described in the imperative tense in complete sentences wherever possible. Avoid usage of phrases such as "could be," "should be," and "would be" throughout the Protocol. Any text that cannot be written in the imperative tense may be added as a "Note." Please include all safety procedures and use of hoods, etc. However, notes should be used sparingly and actions should be described in the imperative tense wherever possible.
We have done our best to convert lines in the protocol to imperative tense.
10. Please add more details to your protocol steps. There should be enough detail in each step to supplement the actions seen in the video so that viewers can easily replicate the protocol. Please ensure you answer the "how" question, i.e., how is the step performed? Alternatively, add references to published material specifying how to perform the protocol action. Some examples:
1.2 and 1.3: Listing an approximate volume to prepare would be helpful.

We have added more details and listed volumes in these parts of the protocol.

6.1: Please use 6.1.1, 6.1.2, 6.1.3, etc., instead of a, b, c, etc. Please write the text in the imperative tense in complete sentences.

We have rewritten section 6 to make these changes.

Steps 8, 9, 12 (including sub-steps): Software steps must be more explicitly explained ('click', 'select', etc.). Please add more specific details (e.g. button clicks for software actions, numerical values for settings, etc.) to your protocol steps.

We have added more details and explanations to software steps.

10.1.1: Please specify incubation temperature.

We have added incubation temperatures.

10.1.2: What volume of NB is used to wash?

We have added a volume to this step.

11. Please include single-line spaces between all paragraphs, headings, steps, etc.

We have made sure to include a space between all Step headings and paragraphs.

12. After you have made all the recommended changes to your protocol (listed above), please re-evaluate your protocol length. There is a 10 page limit for the Protocol. Please revise the protocol section to meet this page limit.

We have double checked that the protocol is not more than 10 pages long.

13. There is a 2.75 page limit for filmable content. Please highlight 2.75 pages or less of the Protocol (including headings and spacing) that identifies the essential steps of the protocol for the video, i.e., the steps that should be visualized to tell the most cohesive story of the Protocol. Remember that non-highlighted Protocol steps will remain in the manuscript, and therefore will still be available to the reader.

We have highlighted full sentences for a total of less than 2.75 pages of highlighted text.

14. Please highlight complete sentences (not parts of sentences). Please ensure that the highlighted part of the step includes at least one action that is written in imperative tense. Please do not highlight any steps describing anesthetization and euthanasia.

We have done this.

15. Please include all relevant details that are required to perform the step in the highlighting. For example: If step 2.5 is highlighted for filming and the details of how to perform the step are given in steps 2.5.1 and 2.5.2, then the sub-steps where the details are provided must be highlighted.

We have done our best to include as many relevant details in the highlighted text as possible without exceeding the page limit.

REVIEWERS' COMMENTS:

Reviewer #1:

Minor Concerns:
One thing that is missing from this paper is a discussion of why they chose the particular calcium indicators for their imaging. It would be nice to add a paragraph discussing the relative advantages and disadvantages of using membrane-targeting calcium indicators instead of soluble indicators –

The membrane localization of GCaMP6s is an important point to highlight and ensure is clear. We have added to our statement in the introduction to expand and clarify why this indicator is important to use:

INTRODUCTION (Lines 138-144)
"This membrane localization positions GCaMP6s in a location to detect *calcium influx through ion channels located in the plasma membrane that are critical for hair-cell function. For example, membrane-localized GCaMP6s can* detect calcium influx through MET channels in apical hair bundles and through $Ca_V1.3$ channels near synaptic ribbons at the base of the cell. *This is in contrast to using GECIs localized in the cytosol; cytosolic GECIs detect calcium signals that are a combination of MET and $Ca_V1.3$ channel activity, as well as calcium contributions from other sources (eg., store release)."*

or other activity dependent indicators (e.g. glusnfr or pHluorins).

We have also added information on other indicators that could be used in this protocol. Based on our experience with other indicators we emphasize why we chose to highlight GCaMP6s-based activity:

DISCUSSION (Lines 1901-1936)
"While this protocol can be adapted and used on many imaging systems, parts of this protocol can also be adapted and used 1) with other indicators besides GCaMP6s and 2) to image activity in other sensory cells and neurons within larval zebrafish. For example, in a previous study, we used this protocol to image activity using multiple genetically encoded indicators within lateral-line hair cells to detect: cytosolic calcium (RGECO1), vesicle fusion (SypHy), membrane voltage (Bongwoori), membrane calcium (jRCaMP1a-caax and GCaMP6s-caax) and within lateral-line afferent processes to detect: membrane calcium (GCaMP6s)[5]. Based on our experience using all of these indicators the transgenic line Tg[myo6b:GCaMP6s-caax] described in this protocol offers an excellent start for imaging activity in lateral-line neuromasts. Of all indicators listed above we have found that GCaMP6s is the most sensitive and photostable. In addition to these features, we highlight the Tg[myo6b:GCaMP6s-caax] transgenic line because it can be used to make two distinct measurements: hair-cell mechanosensation and presynaptic calcium within a single transgenic line."

It also might be helpful to discuss other potential pitfalls and trouble-shooting advice and additional tips and tricks. For example, I could imagine the bungarotoxin injections and fish pinning might be tricky and they may have some wisdom to pass down to novices about these procedures.

In the discussion we have added some alternatives to pinning and alpha-bungarotoxin/heart injections for immobilization and paralysis. It is our hope that the images in the figures help demonstrate our method. Ultimately the challenges with pinning and heart injection are what

motivated this article. We feel that the video recordings of these procedures will be the best way to demonstrate our wisdom and how we actually do these procedures.

Reviewer #2:

Minor Concerns:

I've included a list of comments referencing line numbers. These are minor comments and a few corrections that copy editors may not catch.

The wording is funny here. You could say, "Deflection puts tension on the linkages" rather than "tensions the linkages".
We have made this change.
You may want to state that you are talking about field recording here. It is possible of course to patch onto invidiual cells in the hair bundle, which gives you the "resolution" to look at individual cells, but not a collection of individual cells simultaneously.
We have made a note of the differences between these techniques more clearly the manuscript.
INTRODUCTION (Lines 84-119)
For many years, electrophysiological techniques such as whole-cell patch clamping have been used to probe the functional properties of hair cells *in many species, including zebrafish[15–20]*. These electrophysiological recordings have been particularly valuable to the field of hearing and balance because they can be used to make extremely sensitive measurements from individual sensory cells whose purpose is to encode extremely fast stimuli over a wide range of frequencies and intensities[21, 22]. *Unfortunately, whole-cell recording are unable measure the activity of populations of hair cells. To measure the activity from populations of cells in the zebrafish lateral-line, microphonic potentials and afferent action potentials have been used to detect measure the summed mechanosensitive and postsynaptic response properties of individual neuromasts[23, 24]. Unfortunately, neither whole-cell recordings nor local field potential measurements have the spatial resolution to pinpoint where activity is occurring within an individual cell or measure the activity of each cell within a population.* More recently, calcium dyes and GECIs have been employed to bypass these challenges[25,26].

You many want to briefly discuss why you are using the membrane targeted GCaMP rather than just a cytosolic version, and why you are specifically using the GCaMP6 version.
I think you have good reason to use this specific indicator, and the community should be clear on why it matters.
Great point. We do think that it is important to use the membrane targeted version of GCaMP for these measurements, and we also currently, based on our experience with indicators thus far prefer GCaMP6s for calcium measurements. Please see the parts above that we added for

You might suggest centrifuging the phenol red solution to clear any crystals and prevent them from clogging the heart injection needle.
5.1.   Centrifuge the alpha-bungarotoxin aliquot briefly prior to use to prevent clogging of the heart injection needle. (Lines 415-416)

I'm not really clear on why you need the embryo to be in a special neuronal buffer rather than just E3. Can you discuss that?

Sometime E3 media is not made as accurately and is generally not stored at 4°C or filter sterilized. In addition, from our results we have found that the calcium responses in E3 are smaller as well.
We have added the following note:
Note: 1X E3 can also be used for functional imaging, but responses are more robust and reliable in NB. (Lines 202-203)

A needle polisher could be useful here. Maybe it's worth mentioning.
Great idea.
We have mentioned this in the protocol.
NOTE: A needle polisher can be used to fix jagged breaks. (Line 344)

Add added a pipette polisher to the Table of Materials

You mean 0.35mm (as described above), not nm.
Yes! Thank you, we have made this change.

Possibly labs should always confirm what deflection results in near-saturation of the calcium signal. I don't know what the variability of the calcium signal is if you repeatedly deflect a bundle. If it's relatively low, maybe it's fairly easy to find the saturation point that in your example occurs around a 5um deflection. I wonder if the deflection needed to reach saturation varies among zebrafish strains, since kinocilia length does.
Good point. We have made it more clear that saturation will not always be a 5 μm deflection for every age and indicator. We have added to our original "note".

"NOTE: *Using GCaMP6s in larvae 3 – 7 dpf*, a 5 μm deflection should achieve near saturating GCaMP6s calcium signals and should not damage the apical hair-bundle structures (Figure 3A3''). Smaller displacement distances can be used to deliver non-saturating stimuli (Figure 3A3'). Displacement distances > 10 μm are hard to estimate (Figure 3A3''') and can be damaging over time. *Signal saturation is dependent on age of neuromast (and kinocilial height) as well as the indicator used."* (Lines 835-840)

It seems like binning 2X2 would generally be a good idea since the noise contribution will be

less and you can run at lower laser power. Does not using binning help isolate the separate cells?

Yes, 2X2 binning generally does give better signals because there is less noise and less bleaching due to lower laser setting. The main drawback is that you lose half your resolution. It just depends what you are after. Depending on the resolution of the camera either 1 X or 2 X binning can still separate individual cells. For the camera listed in this protocol 2 X is still good for isolating individual cells. In the representative results we have added the calcium signals in Figure 4 and Figure 5 were acquired at 2 X binning.

We have added to our "note" on binning.
NOTE: Apply 2 X binning if signals are too weak, *noisy*, or have excessive photobleaching. *2 X binning will enhance signal detection at the cost of spatial resolution.* (Lines 856-858 & 996-998)

I think you should present the BAPTA control as simply part of the process, not an optional control.

We made these changes and removed "(optional)"

Just so people aren't confused about how GCaMP works, I would always say that the change in fluorescence IN RESPONSE TO DEFLECTION is gone (in the presence of BAPTA, etc.), not that the signal is gone. People may naively think that chelating calcium causes the GCaMP to be "dark". There is always weak signal from the GCaMP, even in the presence of BAPTA, right?

Good point, we have added detail to Section 10 and 11 to clarify this point.

10.4. Redo Step 8 or 9. After BAPTA treatment *there should be no change in GCaMP6s fluorescence in response to fluid-jet* stimulation in either the apical hair bundles or the synaptic plane. *If changes in GCaMP6s fluorescence persist,* these are not true calcium signals and may be motion artifacts. (Lines 1010-1115)

11.3. Without performing a wash, redo Step 8 or 9. After treatment, *there should still be GCaMP6s fluorescence changes in response to fluid-jet stimulation* in apical hair-bundles but not in the synaptic plane. *If changes in GCaMP6s fluorescence* persist in the synaptic plane, these are not true calcium signals and may be motion artifacts. (Lines 1122-1125)

This is a contentious, but I wonder if a max intensity wouldn't be better than an average intensity projection of the 5 planes. This is a more obvious issue if for example the GCaMP is targeted to an intracellular organelle, since the average projection will average in values from regions where there is no signal, and then effectively drop the dynamic range of the readouts. (Of course, the Max Intensity drops out all the data except the highest signals at each point, which is what people don't like about it.) Maybe a brief mention of the pros and cons of the different types of projections is in order here, but I'll let you decide whether you want to raise that issue. Clearly the average projection works well for this system.

This is a good point. We are going to stick with the average projection as it works best for this analysis. It is true that for our organelle measurements we do use Max intensity projections. This will have to be an adaptation of the protocol.

Similar to the comment above: The GCaMP signal is not eliminated (unless the baseline was set at 0); the response of the signal is eliminated.
We have added more detail to the representative results to make this it more clear that it is the changes in GCaMP6s fluorescence associated with stimulation that are eliminated in the controls.

Figure 1A: This is a trivial thing, but a number of diagrams have this wrong. Are the orientations of the kinocilia correct in relation to the direction of the response? In the figure, you would expect the right and left-of-center cells to respond. I thought the kinocilia mostly face the center of the circle of HC's (central relative to stereocilia), but maybe that's not true.

There is no 100% of the time answer for this question. When there are 6 hair cells the kinocilia are the center of the neuromast and there is a clear line of polarity reversal. In older neuromasts, generally, in the center of the neuromast, the kinocilia are still more commonly central, and face the center of the circle of hair cells. But along the sides of the neuromast bundle orientations are often similar to what we depicted in Figure 1. Because our Figure 1 implies we are in the "center" of a neuromast we have changed the bundle orientation to reflect the bundle orientations that are more commonly depicted in figures in the literature.

By "splaying of the apical hair bundles" I assume you mean splaying of the kinocilia since you cannot usually see the stereocilia. And I assume this must mean that the cupula is broken down. The cupula is something the field tends to ignore, but it's worth mentioning here.

Because we do not know whether the stereocilia are also disrupted when kinocilia are splayed we have modified this statement.

..third, when kinocilia tips splay out in different directions[35]. (Lines 1882-1883)

It is unclear when kinocilia splay if it is due to disruptions in the cupula. It could be, but we are not sure. We do know that if larvae are not maintained and cleaned well that that cupula can be compromised. We added a statement to this effect in our discussion.

A clean aqueous environment is particularly important for young larvae (2 – 4 dpf) or mutants that cannot maintain an upright swimming position and primarily lie on the bottom of the petri dish. In these situations, *lateral-line hair cells and the protective cupula surrounding the hair bundles can easily become compromised*. (Lines 1872-1876)

FIJI Maco